

Proximal Methods for Sparse Optimal Scoring and Discriminant Analysis

Summer Atkins¹, Gudmundur Einarsson², Brendan Ames³, and Line Clemmensen²

¹Department of Mathematics, University of Florida, PO Box 118105, Gainesville, FL 32611-8105, srnatkins@ufl.edu

²Department of Applied Mathematics and Computer Science, Technical University of Denmark, Building 324, 2800 Kongens Lyngby, Denmark, {guei, lkhc}@dtu.dk

³Department of Mathematics, University of Alabama, Box 870350, Tuscaloosa, AL 35487-0350, bpames@ua.edu

December 14, 2024

Abstract

Linear discriminant analysis (LDA) is a classical method for dimensionality reduction, where discriminant vectors are sought to project data to a lower dimensional space for optimal separability of classes. Several recent papers have outlined strategies for exploiting sparsity for using LDA with high-dimensional data. However, many lack scalable methods for solution of the underlying optimization problems. We propose three new numerical optimization schemes for solving the sparse optimal scoring formulation of LDA based on block coordinate descent, the proximal gradient method, and the alternating direction method of multipliers. We show that the per-iteration cost of these methods scales linearly in the dimension of the data provided restricted regularization terms are employed, and cubically in the dimension of the data in the worst case. Furthermore, we establish that if our block coordinate descent framework generates convergent subsequences of iterates, then these subsequences converge to the stationary points of the sparse optimal scoring problem. We demonstrate the effectiveness of our new methods with empirical results for classification of Gaussian data and data sets drawn from benchmarking repositories, including time-series and multispectral X-ray data, and provide `Matlab` and `R` implementations of our optimization schemes.

1 Introduction

Sparse discriminant techniques have become popular in the last decade due to their ability to provide increased interpretation as well as predictive performance for high-dimensional problems where few observations are present. These approaches typically build upon successes from sparse linear regression, in particular the LASSO and its variants (see [Hastie et al. \[2013, Section 3.4.2\]](#) and [Hastie et al. \[2015\]](#)), by augmenting existing schemes for linear discriminant analysis (LDA) with sparsity-inducing regularization terms, such as the ℓ_1 -norm and elastic net.

Thus far, little focus has been put on the optimization strategies of these sparse discriminant methods, nor their computational cost. We propose three novel optimization strategies to obtain discriminant directions in the high-dimensional setting where the number of observations n is much smaller than the ambient dimension p or when features are highly correlated, and prove their convergence. The methods are proposed for multi-class sparse discriminant analysis using the sparse optimal scoring formulation with elastic net penalty proposed in [[Clemmensen et al., 2011](#)]; adding both the ℓ_1 - and ℓ_2 -norm penalties gives sparse solutions which, in particular, are competitive when high correlations exist in feature space due to the grouping behaviour of the ℓ_2 -norm. The first two strategies are proximal gradient methods based on modification of the (fast) iterative shrinkage algorithm [[Beck and Teboulle, 2009](#)] for linear inverse problems. The third method uses a variant of the alternating direction method of multipliers similar to that proposed in [[Ames and Hong, 2016](#)]. We will

see that these heuristics allow efficient classification of high-dimensional data, which was previously impractical using the current state of the art for sparse discriminant analysis. For example, if a diagonal or low-rank Tikhonov regularization term is used and the number of observations is very small relative to p , then the per-iteration cost of each of our algorithms is $\mathcal{O}(p)$; that is, the per-iteration cost of our approach scales linearly with the number of features of our data. Finally, we provide implementations of our algorithms in the form of the R package **accSDA**¹ and Matlab software².

1.1 Existing approaches for sparse LDA

We begin with a brief overview of existing sparse discriminant analysis techniques. Methods such as [Fan and Fan, 2008, Tibshirani et al., 2003, Witten and Tibshirani, 2011] assume independence between the features in the given data. This can lead to poor performance in terms of feature selection as well as predictions, in particular when high correlations exist. Thresholding methods such as [Shao et al., 2011], although proven to be asymptotically optimal, ignore the existing multi-linear correlations when thresholding low correlation estimates. Thresholding, furthermore, does not guarantee an invertible correlation matrix, and often pseudo-inverses must be utilized.

For two-class problems, the results of [Mai and Zou, 2013] established an equivalence between the three methods described in [Clemmensen et al., 2011, Mai et al., 2012, Wu et al., 2008]. These three approaches are formulated as constrained versions of the Fisher’s discriminant problem, the optimal scoring problem, and a least squares formulation of linear discriminant analysis, respectively. For scaled regularization parameters, [Mai and Zou, 2013] showed that they all behave asymptotically as Bayes rules. Another two-class sparse linear discriminant method is the linear programming discriminant method proposed in [Cai and Liu, 2011], which finds an ℓ_1 -norm penalized estimate of the product between covariance matrix and difference in means.

The sparse optimal scoring (SOS) problem was originally formulated in [Clemmensen et al., 2011] as a multi-class problem seeking at most $K - 1$ sparse discriminating directions, whereas [Mai and Zou, 2013] was formulated for binary problems. Mai and Zou later proposed a multi-class sparse discriminant analysis (MSDA) based on the Bayes rule formu-

lation of linear discriminant analysis in [Mai and Zou, 2015]. It imposes only the ℓ_1 -norm penalty, whereas the SOS imposes an elastic net penalty (ℓ_1 - plus ℓ_2 -norm). Adding the ℓ_2 -norm can give better predictive performance, in particular when very high correlations exist in data. MSDA, furthermore, finds all discriminative directions at once, whereas SOS finds them sequentially via deflation. A sequential solution can be an advantage if the number of classes is high, and a solution involving only a few directions (the most discriminating ones) is needed. On the other hand, if K is small, finding all directions at once, may be advantageous, in order to not propagate errors in a sequential manner.

Finally, the zero-variance sparse discriminant analysis approach of [Ames and Hong, 2016] reformulates the sparse discriminant analysis problem as an ℓ_1 -penalized nonconvex optimization problem in order to sequentially identify discriminative directions in the null-space of the pooled within-class scatter matrix. Most relevant for our discussion here is the use of proximal methods to approximately solve the nonconvex optimization problems in [Ames and Hong, 2016]; we will adopt a similar approach for solving the SOS problem.

2 Proximal Methods for Sparse Discriminant Analysis

In this section, we describe a block coordinate descent approach for (approximately) solving the sparse optimal scoring problem for linear discriminant analysis. Proposed in [Hastie et al., 1994], the optimal scoring problem recasts linear discriminant analysis as a generalization of linear regression where both the response variable, corresponding to an optimal labeling or scoring of the classes, and linear model parameters, which yield the discriminant vector, are sought. Specifically, suppose that we have $n \times p$ data matrix \mathbf{X} , where the rows of \mathbf{X} correspond to observations in \mathbf{R}^p sampled from one of K classes; we assume that the data has been centered so that the sample mean is the zero vector $\mathbf{0} \in \mathbf{R}^p$. Optimal scoring generates a sequence of discriminant vectors and conjugate scoring vectors as follows. Suppose that we have identified the first $k - 1$ discriminant vectors $\beta_1, \dots, \beta_{k-1} \in \mathbf{R}^p$ and scoring vectors $\theta_1, \dots, \theta_{k-1} \in \mathbf{R}^K$. To calculate the k th discriminant vector β_k and scoring vector θ_k , we solve the

¹Available at <https://github.com/gumeo/accSDA> and <https://cran.r-project.org/web/packages/accSDA>

²Available at <http://bpames.people.ua.edu/software>

optimal scoring criterion problem

$$\begin{aligned} \arg \min_{\boldsymbol{\theta} \in \mathbf{R}^K, \boldsymbol{\beta} \in \mathbf{R}^p} \quad & \|\mathbf{Y}\boldsymbol{\theta} - \mathbf{X}\boldsymbol{\beta}\|^2 \\ \text{s.t.} \quad & \frac{1}{n}\boldsymbol{\theta}^T \mathbf{Y}^T \mathbf{Y} \boldsymbol{\theta} = 1, \\ & \boldsymbol{\theta}^T \mathbf{Y}^T \mathbf{Y} \boldsymbol{\theta}_\ell = 0 \quad \forall \ell < k, \end{aligned} \quad (1)$$

where \mathbf{Y} denotes the $n \times K$ indicator matrix for class membership, defined by $y_{ij} = 1$ if the i th observation belongs to the j th class, and $y_{ij} = 0$ otherwise, and $\|\cdot\| : \mathbf{R}^n \rightarrow \mathbf{R}$ denotes the vector ℓ_2 -norm on \mathbf{R}^n defined by $\|\mathbf{y}\| = \sqrt{y_1^2 + y_2^2 + \dots + y_n^2}$ for all $\mathbf{y} \in \mathbf{R}^n$. We direct the reader to [Hastie et al., 1994] for further details regarding the derivation of (1).

A variant of the optimal scoring problem which employs regularization via the elastic net penalty function is proposed in [Clemmensen et al., 2011]. As before, suppose that we have identified the first $k-1$ discriminant vectors $\boldsymbol{\beta}_1, \dots, \boldsymbol{\beta}_{k-1}$ and scoring vectors $\boldsymbol{\theta}_1, \dots, \boldsymbol{\theta}_{k-1}$. To calculate the k th sparse discriminant vector $\boldsymbol{\beta}_k$ and scoring vector $\boldsymbol{\theta}_k$, as the optimal solutions of the optimal scoring criterion problem

$$\begin{aligned} \arg \min_{\boldsymbol{\theta} \in \mathbf{R}^K, \boldsymbol{\beta} \in \mathbf{R}^p} \quad & \|\mathbf{Y}\boldsymbol{\theta} - \mathbf{X}\boldsymbol{\beta}\|^2 + \gamma \boldsymbol{\beta}^T \boldsymbol{\Omega} \boldsymbol{\beta} + \lambda \|\boldsymbol{\beta}\|_1 \\ \text{s.t.} \quad & \frac{1}{n}\boldsymbol{\theta}^T \mathbf{Y}^T \mathbf{Y} \boldsymbol{\theta} = 1, \\ & \boldsymbol{\theta}^T \mathbf{Y}^T \mathbf{Y} \boldsymbol{\theta}_\ell = 0 \quad \forall \ell < k, \end{aligned} \quad (2)$$

where $\mathbf{Y} \in \mathbf{R}^{n \times K}$ is again the indicator matrix for class membership, λ and γ are nonnegative tuning parameters, $\boldsymbol{\Omega}$ is a $p \times p$ positive definite matrix, and $\|\cdot\|_1 : \mathbf{R}^p \rightarrow \mathbf{R}$ denotes the vector ℓ_1 -norm on \mathbf{R}^p defined by $\|\mathbf{x}\|_1 = |x_1| + |x_2| + \dots + |x_p|$ for all $\mathbf{x} \in \mathbf{R}^p$. That is, (2) is the result of adding regularization to the optimal scoring problem using a linear combination of the Tikhonov penalty term $\boldsymbol{\beta}^T \boldsymbol{\Omega} \boldsymbol{\beta}$ and the ℓ_1 -norm penalty $\|\boldsymbol{\beta}\|_1$; we will provide further discussion regarding the choice of $\boldsymbol{\Omega}$ in Section 2.4. The optimization problem (2) is nonconvex, due to the presence of nonconvex spherical constraints. As such, we do not expect to find a globally optimal solution of (2) using iterative methods. In [Clemmensen et al., 2011], a block coordinate descent method to iteratively approximate solutions of (2) is proposed. Specifically, suppose that we have an estimate $(\boldsymbol{\theta}^t, \boldsymbol{\beta}^t)$ of $(\boldsymbol{\theta}_k, \boldsymbol{\beta}_k)$. To update $\boldsymbol{\theta}^t$, we fix $\boldsymbol{\beta} = \boldsymbol{\beta}^t$ and solve the optimization problem

$$\begin{aligned} \boldsymbol{\theta}^{t+1} = \arg \min_{\boldsymbol{\theta} \in \mathbf{R}^K} \quad & \|\mathbf{Y}\boldsymbol{\theta} - \mathbf{X}\boldsymbol{\beta}^t\|^2 \\ \text{s.t.} \quad & \frac{1}{n}\boldsymbol{\theta}^T \mathbf{Y}^T \mathbf{Y} \boldsymbol{\theta} = 1, \\ & \boldsymbol{\theta}^T \mathbf{Y}^T \mathbf{Y} \boldsymbol{\theta}_\ell = 0 \quad \forall \ell < k. \end{aligned} \quad (3)$$

The subproblem (3) is nonconvex in $\boldsymbol{\theta}$, however, it is known that (3) admits an analytic solution and can be solved exactly in polynomial time (see Clemmensen et al. [2011, Section 2.2] for more details). Indeed, we have the following lemma.

Algorithm 1: Block Coordinate Descent for SDA (2)

Data: Given initial iterate $\boldsymbol{\theta}^0 \in \mathbf{R}^K$

Data: Approximate solution $(\boldsymbol{\theta}^*, \boldsymbol{\beta}^*)$ of (2).

for $t = 0, 1, 2 \dots$ *until converged*

Update $\boldsymbol{\beta}^t$ as the solution of (5) with $\boldsymbol{\theta} = \boldsymbol{\theta}^t$ using the solution returned by one of Algorithm 3, Algorithm 4, Algorithm 5, or Algorithm 6.

Update $\boldsymbol{\theta}^{t+1}$ by

$$\begin{aligned} \mathbf{w} &= (\mathbf{I} - \mathbf{Q}_k \mathbf{Q}_k^T \mathbf{D}) \mathbf{D}^{-1} \mathbf{Y}^T \mathbf{X} \boldsymbol{\beta}^t, \\ \boldsymbol{\theta}^{t+1} &= \frac{\mathbf{w}}{\sqrt{\mathbf{w}^T \mathbf{D} \mathbf{w}}} \end{aligned}$$

end

Lemma 2.1 *The problem (3) has optimal solution*

$$\boldsymbol{\theta}^{t+1} = s(\mathbf{I} - \mathbf{Q}_k \mathbf{Q}_k^T \mathbf{D}) \mathbf{D}^{-1} \mathbf{Y}^T \mathbf{X} \boldsymbol{\beta}^t, \quad (4)$$

where $\mathbf{D} = \frac{1}{n} \mathbf{Y}^T \mathbf{Y}$, \mathbf{Q}_k is the $K \times k$ matrix with columns consisting of the $k-1$ scoring vectors $\boldsymbol{\theta}_1, \dots, \boldsymbol{\theta}_{k-1}$ and the all-ones vector $\mathbf{e} \in \mathbf{R}^K$, and s is a proportionality constant ensuring that $(\boldsymbol{\theta}^{t+1})^T \mathbf{D} \boldsymbol{\theta}^{t+1} = 1$.

For completeness, we provide a proof of Lemma 2.1 in Appendix A. After we have updated $\boldsymbol{\theta}^{t+1}$, we obtain $\boldsymbol{\beta}^{t+1}$ by solving the unconstrained optimization problem

$$\boldsymbol{\beta}^{t+1} = \arg \min_{\boldsymbol{\beta} \in \mathbf{R}^p} \|\mathbf{Y}\boldsymbol{\theta}^{t+1} - \mathbf{X}\boldsymbol{\beta}\|^2 + \gamma \boldsymbol{\beta}^T \boldsymbol{\Omega} \boldsymbol{\beta} + \lambda \|\boldsymbol{\beta}\|_1. \quad (5)$$

That is, we update $\boldsymbol{\beta}^{t+1}$ by solving the generalized elastic net problem (5). It is suggested in [Clemmensen et al., 2011] that (2) can be solved using the algorithm proposed in [Zou and Hastie, 2005]. Unfortunately, this approach carries a per-iteration computational cost on the order of $\mathcal{O}(mnp + m^3)$, where m is the desired number of nonzero coefficients, which is prohibitively expensive if both p and m are large; for example, if $m = cp$ for some constant $c \in (0, 1)$, then the per-iteration cost scales cubically with p .

Our primary contribution is a collection of algorithms for solving the elastic net problem (5). Specifically, we propose three new algorithms, each based on the evaluation of proximal operators. We will see that these algorithms require significantly fewer computational resources than the elastic net algorithm if we exploit structure in the regularization parameter $\boldsymbol{\Omega}$.

2.1 Proximal Algorithms for the Generalized Elastic Net Problem

Given a convex function $f : \mathbf{R}^p \rightarrow \mathbf{R}$, the *proximal operator* $\text{prox}_f : \mathbf{R}^p \rightarrow \mathbf{R}^p$ of f is defined by

$$\text{prox}_f(\mathbf{y}) = \arg \min_f \left\{ f(\mathbf{x}) + \frac{1}{2} \|\mathbf{x} - \mathbf{y}\|^2 \right\},$$

which yields a point that balances the competing objectives of being near \mathbf{y} while simultaneously minimizing f . The use of proximal operators is a classical technique in optimization, particularly as surrogates for gradient descent steps for minimization of nonsmooth functions. For example, consider the optimization problem

$$\min_{\mathbf{x} \in \mathbf{R}^p} f(\mathbf{x}) + g(\mathbf{x}), \quad (6)$$

where $f : \mathbf{R}^p \rightarrow \mathbf{R}$ is differentiable and $g : \mathbf{R}^p \rightarrow \mathbf{R}$ is potentially nonsmooth. That is, (6) minimizes an objective that can be decomposed as the sum of a differentiable function f and nonsmooth function g . To solve (6), the *proximal gradient method* performs iterations consisting of a step in the direction of the negative gradient $-\nabla f$ of the smooth part f followed by evaluation of the proximal operator of g : given iterate \mathbf{x}^t , we obtain the updated iterate \mathbf{x}^{t+1} by

$$\mathbf{x}^{t+1} = \text{prox}_{\alpha_t g}(\mathbf{x}^t - \alpha_t \nabla f(\mathbf{x}^t)), \quad (7)$$

where α_t is a step length parameter. If both f and g are differentiable and the step size α_t is small, then this approach reduces to the classical gradient descent iteration: $\mathbf{x}^{t+1} \approx \mathbf{x}^t - \alpha_t \nabla f(\mathbf{x}^t) - \alpha_t \nabla g(\mathbf{x}^t)$. We direct the reader to the recent survey article [Parikh and Boyd, 2014] for more details regarding the proximal gradient method and proximal operators in general.

In [Beck and Teboulle, 2009], the authors consider a specialization of the proximal gradient method, called the *iterative soft-thresholding algorithm (ISTA)* to the ℓ_1 -regularized linear inverse problem

$$\min_{\mathbf{x} \in \mathbf{R}^n} \|\mathbf{A}\mathbf{x} - \mathbf{b}\|^2 + \lambda \|\mathbf{x}\|_1, \quad (8)$$

where $\mathbf{A} \in \mathbf{R}^{m \times n}$, $\mathbf{b} \in \mathbf{R}^m$ are known, and $\lambda > 0$ is a regularization parameter chosen by the user; here \mathbf{b} is often noisy measurements of an unknown vector or signal \mathbf{x} by the sampling matrix \mathbf{A} . The primary contribution of [Beck and Teboulle, 2009] is an accelerated variant of ISTA, called *fast iterative soft-threshold (FISTA)*, and a convergence analysis establishing the non-asymptotic global rate of convergence of both ISTA and FISTA; we'll delay further

Algorithm 2: Backtracking algorithm for ISTA

Data: Start with $L_0 > 0$ and scaling parameter $\eta > 1$

Result: Minimizer \mathbf{x}^* of F .

for $t = 0, 1, 2 \dots$ *until converged*

for $k = 0, 1, 2 \dots$ *until step size accepted*

 Update step length

$$\bar{L} = \eta^k L_{t-1}, \quad \alpha = \frac{1}{\bar{L}}$$

 Update iterate using proximal gradient step (7):

$$\mathbf{x}^{t+1} = \text{prox}_{\alpha g}(\mathbf{x}^t + \bar{\alpha} \nabla f(\mathbf{x}^t))$$

 Determine whether to accept update or increment step length:

if $F(\mathbf{x}^{t+1}) \leq f(\mathbf{x}^t) + \nabla f(\mathbf{x}^t)^T (\mathbf{x}^{t+1} - \mathbf{x}^t) + \frac{\bar{L}}{2} \|\mathbf{x}^{t+1} - \mathbf{x}^t\|^2 + g(\mathbf{x}^{t+1})$

 Accept update: $L_t = \bar{L}$, $\alpha_t = \bar{\alpha}$.

break.

end

end

end

discussion of FISTA until Section 2.2. Although motivated by the linear inverse problem (8), the analysis of [Beck and Teboulle, 2009] focuses on the more general problem of minimizing the sum $f + g$, where f is differentiable with Lipschitz continuous gradient and g is potentially nonsmooth. In this case, a Lipschitz constant of ∇f is used as a constant step size in (7) or the step length is chosen using the backtracking rule given by Algorithm 2. The following theorem establishes that the sequence of iterates generated converges sublinearly to the optimal function value of $F := f + g$ at a rate no worse than $\mathcal{O}(1/t)$; see [Beck and Teboulle, 2009, Theorem 3.1].

Theorem 2.1 *Let the function $F : \mathbf{R}^n \rightarrow \mathbf{R}$ be decomposable as $F(\mathbf{x}) = f(\mathbf{x}) + g(\mathbf{x})$, where f is differentiable with Lipschitz continuous gradient; let L be a Lipschitz constant such that*

$$\|\nabla f(\mathbf{x}) - \nabla f(\mathbf{y})\| \leq L \|\mathbf{x} - \mathbf{y}\|$$

for all $\mathbf{x}, \mathbf{y} \in \mathbf{R}^n$. Suppose that F has minimizer $\mathbf{x}^ \in \mathbf{R}^n$. Let $\{\mathbf{x}^t\}_{t=0}^\infty$ be the sequence of iterates generated by (7) with constant step size $\alpha = 1/L$ or by Algorithm 2. Then there exists constant $c > 0$ such that*

$$F(\mathbf{x}^t) - F(\mathbf{x}^*) \leq \frac{cL \|\mathbf{x}^0 - \mathbf{x}^*\|^2}{t} \quad (9)$$

for all t .

Expanding the residual norm term $\|\mathbf{Y}\boldsymbol{\theta} - \mathbf{X}\boldsymbol{\beta}\|^2$ in the objective of (5) and dropping the constant term shows that (5) is equivalent to minimizing

$$F(\boldsymbol{\beta}) = \frac{1}{2}\boldsymbol{\beta}^T \mathbf{A}\boldsymbol{\beta} + \mathbf{d}^T \boldsymbol{\beta} + \lambda\|\boldsymbol{\beta}\|_1, \quad (10)$$

where $\mathbf{A} = 2(\mathbf{X}^T \mathbf{X} + \gamma\boldsymbol{\Omega})$ and $\mathbf{d} = -2\mathbf{X}^T \mathbf{Y}\boldsymbol{\theta}^{t+1}$. We can decompose F as $F(\boldsymbol{\beta}) = f(\boldsymbol{\beta}) + g(\boldsymbol{\beta})$, where $f(\boldsymbol{\beta}) = \frac{1}{2}\boldsymbol{\beta}^T \mathbf{A}\boldsymbol{\beta} + \mathbf{d}^T \boldsymbol{\beta}$ and $g(\boldsymbol{\beta}) = \lambda\|\boldsymbol{\beta}\|_1$. Note that F is strongly convex if the penalty matrix $\boldsymbol{\Omega}$ is positive definite; in this case (10) has unique minimizer. Note further that f is differentiable with

$$\nabla f(\boldsymbol{\beta}) = \mathbf{A}\boldsymbol{\beta} + \mathbf{d}.$$

Moreover, the proximal operator of the ℓ_1 -norm term $g(\boldsymbol{\beta}) = \lambda\|\boldsymbol{\beta}\|_1$ is given by

$$\text{prox}_{\lambda\|\cdot\|_1}(\mathbf{y}) = \text{sign}(\mathbf{y}) \max\{|\mathbf{y}| - \lambda\mathbf{e}, \mathbf{0}\} =: S_\lambda(\mathbf{y});$$

see [Parikh and Boyd, 2014, Section 6.5.2]. The proximal operator $S_\lambda = \text{prox}_{\lambda\|\cdot\|_1}$ is often called the *soft thresholding operator* (with respect to the threshold λ) and $\text{sign} : \mathbf{R}^p \rightarrow \mathbf{R}^p$ and $\max : \mathbf{R}^p \times \mathbf{R}^p \rightarrow \mathbf{R}^p$ are the element-wise sign and maximum mappings defined by

$$[\text{sign}(\mathbf{y})]_i = \text{sign}(y_i) = \begin{cases} +1, & \text{if } y_i > 0 \\ 0, & \text{if } y_i = 0 \\ -1, & \text{if } y_i < 0 \end{cases}$$

and $[\max(\mathbf{x}, \mathbf{y})]_i = \max(x_i, y_i)$. Using this decomposition, we can apply the proximal gradient method to generate a sequence of iterates $\{\boldsymbol{\beta}^t\}$ by

$$\boldsymbol{\beta}^{t+1} = \text{sign}(\mathbf{p}^t) \max\{|\mathbf{p}^t| - \lambda\alpha_t \mathbf{e}, \mathbf{0}\}, \quad (11)$$

where

$$\mathbf{p}^t = \boldsymbol{\beta}^t - \alpha_t \nabla f(\boldsymbol{\beta}^t) = \boldsymbol{\beta}^t - \alpha_t (\mathbf{A}\boldsymbol{\beta}^t + \mathbf{d}); \quad (12)$$

here, \mathbf{e} and $\mathbf{0}$ denote the all-ones and all-zeros vectors in \mathbf{R}^p , respectively. Our proximal gradient algorithm is summarized in Algorithm 3. It is important to note that this update scheme is virtually identical to that of the *iterative soft thresholding algorithm (ISTA)* for linear inverse problems (see Beck and Teboulle [2009]). Here, our problem and update formula differs only from that typically associated with ISTA in the presence of the Tikhonov regression term $\boldsymbol{\beta}^T \boldsymbol{\Omega} \boldsymbol{\beta}$ in our model. As an immediate consequence, we see that the sequence of function values $\{F(\boldsymbol{\beta}^t)\}$ generated by Algorithm 3, with an appropriate choice of step lengths $\{\alpha_t\}$, converges sublinearly to the optimal function value of (10) at a rate no worse than $\mathcal{O}(1/t)$ (compare to Beck and Teboulle [2009, Theorem 3.1]).

Algorithm 3: Proximal gradient method for solving the elastic net subproblem (5)

Data: Initial iterate $\boldsymbol{\beta}^0$ and sequence of step lengths $\{\alpha_t\}_{t=0}^\infty$.

Result: Solution $\boldsymbol{\beta}^*$ of (5).

for $t = 0, 1, 2 \dots$ *until converged*

Update gradient term by (12):

$$\mathbf{p}^t = \boldsymbol{\beta}^t - \alpha_t (\mathbf{A}\boldsymbol{\beta}^t + \mathbf{d}).$$

Update iterate using proximal gradient step (11):

$$\boldsymbol{\beta}^{t+1} = \text{sign}(\mathbf{p}^t) \max\{|\mathbf{p}^t| - \lambda\alpha_t \mathbf{e}, \mathbf{0}\}$$

end

Theorem 2.2 *Let $\{\boldsymbol{\beta}^t\}$ be generated by Algorithm 3 with initial iterate $\boldsymbol{\beta}^0$ and constant step size $\alpha_t = \alpha \in (0, 1/\|\mathbf{A}\|)$ or step sizes chosen using the backtracking scheme given by Algorithm 2, where $\|\mathbf{A}\| = \lambda_{\max}(\mathbf{A})$ denotes the spectral norm of \mathbf{A} equal to the largest magnitude eigenvalue of \mathbf{A} . Suppose that $\boldsymbol{\beta}^*$ is a minimizer of F . Then there exists constant c such that*

$$F(\boldsymbol{\beta}^t) - F(\boldsymbol{\beta}^*) \leq \frac{c\|\mathbf{A}\|\|\boldsymbol{\beta}^0 - \boldsymbol{\beta}^*\|^2}{t} \quad (13)$$

for any $t \geq 1$.

As an immediate consequence of Theorem 2.2, the sequence of iterates generated by Algorithm 3 converges to the unique minimizer of (5) if the penalty parameter $\boldsymbol{\Omega}$ is chosen to be positive definite. Indeed, in this case, the sequence of iterates $\{\boldsymbol{\beta}^t\}$ converges to a solution with optimal value; since strongly convex functions have unique minimizers, $\{\boldsymbol{\beta}^t\}$ must converge to $\boldsymbol{\beta}^*$. If we choose $\boldsymbol{\Omega}$ to be positive semidefinite, then any limit point of the sequence of iterates generated by Algorithm 3 is a minimizer of (5); we will see that using such a matrix may have attractive computational advantages despite this loss of uniqueness.

It is reasonably easy to see that the quadratic term of F is differentiable and has Lipschitz continuous gradient with constant $L = \|\mathbf{A}\|$; this is the significance of the $\|\mathbf{A}\|$ term in (13). In order to ensure convergence in our proximal gradient method, we need to estimate $\|\mathbf{A}\|$ to choose a sufficiently small step size α . Computing this Lipschitz constant may be prohibitively expensive for large p ; one can typically calculate $\|\mathbf{A}\|$ to arbitrary precision using variants of the Power Method (see Golub and Van Loan [2013, Sections 7.3.1, 8.2]) at a cost of $\mathcal{O}(p^2 \log p)$ float-

ing point operations. Instead, we could use an upper bound $\tilde{L} \geq L$ to compute our constant step size $\alpha = 1/\tilde{L} \leq 1/L$. For example, when $\mathbf{\Omega}$ is a diagonal matrix, we estimate $\|\mathbf{A}\|$ by

$$\begin{aligned} \|\mathbf{A}\| &= 2\|\gamma\mathbf{\Omega} + \mathbf{X}^T\mathbf{X}\| \\ &\leq 2\gamma\|\text{diag}(\mathbf{\Omega})\|_\infty + 2\|\mathbf{X}\|_F^2 \approx \frac{1}{\alpha}, \end{aligned}$$

where $\text{diag}(\mathbf{M}) \in \mathbf{R}^p$ is the vector of diagonal entries of the matrix $\mathbf{M} \in \mathbf{R}^{p \times p}$. Here, we used the triangle inequality and the identity $\|\mathbf{X}^T\mathbf{X}\| \leq \|\mathbf{X}\|_F^2$, where $\|\mathbf{X}\|_F$ denotes the Frobenius norm of \mathbf{X} defined by

$$\|\mathbf{X}\|_F = \sqrt{\sum_{i=1}^n \sum_{j=1}^p x_{ij}^2}.$$

The Frobenius norm and, hence, this estimate of $\|\mathbf{A}\|$ can be computed using only $\mathcal{O}(np)$ floating point operations.

2.2 The Accelerated Proximal Gradient Method

The similarity of our method to iterative soft thresholding and, more generally, our use of proximal gradient steps to mimic the gradient method for minimization of our nonsmooth objective, suggests that we may be able to use momentum terms to accelerate convergence of our iterates. In particular, we modify the fast iterative soft thresholding algorithm (FISTA) described in [Beck and Teboulle, 2009, Section 4] to solve our subproblem. This approach extends a variety of accelerated gradient descent methods, most notably those of Nesterov [Nesterov, 1983, 2005, 2013], to minimization of composite convex functions; for further details regarding the acceleration process and motivation for why such acceleration is possible, we direct the reader to the references [Allen-Zhu and Orecchia, 2014, Bubeck et al., 2015, Flammarion and Bach, 2015, Lessard et al., 2016, O’Donoghue and Candes, 2015, Su et al., 2014, Tseng, 2008].

We accelerate convergence of our iterates by taking a proximal gradient step from an extrapolation of the last two iterates. Applied to (6), the accelerated proximal gradient method features updates of the form

$$\mathbf{y}^{t+1} = \mathbf{x}^t + \omega_t(\mathbf{x}^t - \mathbf{x}^{t-1}) \quad (14)$$

$$\mathbf{x}^{t+1} = \text{prox}_{\alpha g}(\mathbf{y}^{t+1} - \alpha \nabla f(\mathbf{y}^{t+1})), \quad (15)$$

where $\omega_t \in [0, 1)$ is an extrapolation parameter; a standard choice of this parameter is $t/(t+3)$. Applying this modification to our original proximal gradient

Algorithm 4: Accelerated proximal gradient method for solving (5) with constant step size

Data: Initial iterates $\beta^0 = \beta^{-1}$, step length α , and sequence of extrapolation parameters $\{\omega_t\}_{t=0}^\infty$.

Result: Solution β^* of (5).

for $t = 0, 1, 2 \dots$ *until converged*

Update momentum term by (14):

$$\mathbf{y}^t = \beta^t + \omega_t(\beta^t - \beta^{t-1}).$$

Update gradient term by (12):

$$\mathbf{p}^t = \mathbf{y}^t - \alpha(\mathbf{A}\mathbf{y}^t + \mathbf{d}).$$

Update iterate using proximal gradient step (11):

$$\beta^{t+1} = \text{sign}(\mathbf{p}^t) \max\{|\mathbf{p}^t| - \lambda\alpha\mathbf{e}, \mathbf{0}\}.$$

end

algorithm yields Algorithm 4. Modifying the backtracking line search of Algorithm 2 to use the accelerated proximal gradient update yields Algorithm 5. It can be shown that the sequence of iterates generated by either of these algorithms converges in value to the optimal solution of (5) at rate $\mathcal{O}(1/t^2)$ (see Beck and Teboulle [2009, Theorem 4.4]).

Theorem 2.3 *Let $\{\beta^t\}$ be generated by Algorithm 4 with initial iterate β^0 and constant step size $\alpha_t = \alpha \in (0, 1/\|\mathbf{A}\|)$. Then there exists constant $C > 0$ such that*

$$F(\beta^t) - F(\beta^*) \leq \frac{C\|\mathbf{A}\|\|\beta^0 - \beta^*\|^2}{t^2} \quad (16)$$

for any $t \geq 1$ and minimizer β^* of F .

2.3 The Alternating Direction Method of Multipliers

We conclude by proposing a third algorithm for minimization of (10) based on the *alternating direction method of multipliers* (ADMM) for minimizing separable functions under linear coupling constraints. The ADMM solves problems of the form

$$\min_{\mathbf{x} \in \mathbf{R}^p, \mathbf{y} \in \mathbf{R}^m} \{f(\mathbf{x}) + g(\mathbf{y}) : \mathbf{A}\mathbf{x} + \mathbf{B}\mathbf{y} = \mathbf{c}\}, \quad (17)$$

via an approximate dual gradient ascent, where $f : \mathbf{R}^p \rightarrow \mathbf{R}$, $g : \mathbf{R}^m \rightarrow \mathbf{R}$, $\mathbf{A} \in \mathbf{R}^{r \times p}$, $\mathbf{B} \in \mathbf{R}^{r \times m}$,

Algorithm 5: Accelerated proximal gradient method for solving (5) with backtracking line search

Data: Initial iterates $\beta^0 = \beta^{-1}$, initial Lipschitz constant $L_0 > 0$, scaling parameter $\eta > 1$, and sequence of extrapolation parameters $\{\omega_t\}_{t=0}^\infty$.

Result: Solution β^* of (5).

for $t = 0, 1, 2 \dots$ until converged

 for $k = 0, 1, 2 \dots$ until step size accepted

 Update step length

$$\bar{L} = \eta^k L_{t-1}, \quad \alpha = \frac{1}{\bar{L}}$$

 Update iterate using accelerated proximal gradient step (11):

$$\mathbf{y}^t = \beta^t + \omega_t(\beta^t - \beta^{t-1})$$

$$\mathbf{p}^t = \mathbf{y}^t - \alpha(\mathbf{A}\mathbf{y}^t + \mathbf{d})$$

$$\beta^{t+1} = \text{sign}(\mathbf{p}^t) \max\{|\mathbf{p}^t| - \lambda\alpha\mathbf{e}, \mathbf{0}\}.$$

 Determine whether to accept update or increment step length:

 if $(\beta^{t+1} - \mathbf{y}^{t+1})^T \left(\frac{\bar{L}}{2} \mathbf{I} - \mathbf{A} \right) (\beta^{t+1} - \mathbf{y}^{t+1}) \geq 0$

 Accept update: set $L_t = \bar{L}$ and $\alpha_t = \bar{\alpha}$.

 break.

 end

 end

end

and $\mathbf{c} \in \mathbf{R}^r$; we direct the reader to the recent survey [Boyd et al., 2011] for more details regarding the ADMM.

Recall that the minimization of the composite function F defined in (10) can be written as the unconstrained optimization problem

$$\min_{\beta \in \mathbf{R}^p} F(\beta) = \min_{\beta \in \mathbf{R}^p} \frac{1}{2} \beta^T \mathbf{A} \beta + \mathbf{d}^T \beta + \lambda \|\beta\|_1. \quad (18)$$

We can rewrite (18) in an equivalent form appropriate for the ADMM by splitting the decision variable $\beta \in \mathbf{R}^p$ as two new variables $\mathbf{x}, \mathbf{y} \in \mathbf{R}^p$ with an accompanying linear coupling constraint $\mathbf{x} = \mathbf{y}$. Under this change of variables, we can express (18) as

$$\begin{aligned} \min_{\mathbf{x}, \mathbf{y} \in \mathbf{R}^p} \quad & \frac{1}{2} \mathbf{x}^T \mathbf{A} \mathbf{x} - \mathbf{x}^T \mathbf{d} + \lambda \|\mathbf{y}\|_1 \\ \text{s.t.} \quad & \mathbf{x} - \mathbf{y} = \mathbf{0}. \end{aligned} \quad (19)$$

The ADMM generates a sequence of iterates using ap-

proximate dual gradient ascent steps as follows. The augmented Lagrangian of (19) is defined by

$$\begin{aligned} L_\mu(\mathbf{x}, \mathbf{y}, \mathbf{z}) = & \frac{1}{2} \mathbf{x}^T \mathbf{A} \mathbf{x} - \mathbf{x}^T \mathbf{d} + \lambda \|\mathbf{y}\|_1 \\ & + \mathbf{z}^T (\mathbf{x} - \mathbf{y}) + \frac{\mu}{2} \|\mathbf{x} - \mathbf{y}\|^2 \end{aligned}$$

for all $\mathbf{x}, \mathbf{y}, \mathbf{z} \in \mathbf{R}^p$; here, $\mu > 0$ is a penalty parameter controlling the emphasis on enforcing feasibility of the primal iterates \mathbf{x} and \mathbf{y} . To approximate the gradient of the dual functional of (19), we alternately minimize the augmented Lagrangian with respect to \mathbf{x} and \mathbf{y} . We then update the dual variable \mathbf{z} by a dual ascent step using this approximate gradient.

Suppose that we have the iterates $(\mathbf{x}^t, \mathbf{y}^t, \mathbf{z}^t)$ after t steps of our algorithm. To update \mathbf{x} , we take

$$\begin{aligned} \mathbf{x}^{t+1} &= \arg \min_{\mathbf{x} \in \mathbf{R}^p} L_\mu(\mathbf{x}, \mathbf{y}^t, \mathbf{z}^t) \\ &= \arg \min_{\mathbf{x} \in \mathbf{R}^p} \frac{1}{2} \mathbf{x}^T (\mu \mathbf{I} + \mathbf{A}) \mathbf{x} - \mathbf{x}^T (\mathbf{d} + \mu \mathbf{y}^t - \mathbf{z}^t). \end{aligned}$$

Applying the first order necessary and sufficient conditions for optimality, we see that \mathbf{x}^{t+1} must satisfy

$$(\mu \mathbf{I} + \mathbf{A}) \mathbf{x}^{t+1} = \mathbf{d} + \mu \mathbf{y}^t - \mathbf{z}^t. \quad (20)$$

Thus, \mathbf{x}^{t+1} is obtained as the solution of a linear system. Note that the coefficient matrix $\mu \mathbf{I} + \mathbf{A}$ is independent of t ; we take the Cholesky decomposition of $\mu \mathbf{I} + \mathbf{A} = \mathbf{B} \mathbf{B}^T$ during a preprocessing step and obtain \mathbf{x}^{t+1} by solving the two triangular systems given by

$$\mathbf{B} \mathbf{B}^T \mathbf{x}^{t+1} = \mathbf{d} + \mu \mathbf{y}^t - \mathbf{z}^t.$$

When the generalized elastic net matrix $\mathbf{\Omega}$ is diagonal, or $\mathbf{M} := \mu \mathbf{I} + 2\gamma \mathbf{\Omega}$ is otherwise easy to invert, we can invoke the Sherman-Morrison-Woodbury formula (see Golub and Van Loan [2013, Section 2.1.4]) to solve this linear system more efficiently; more details will be provided in Section 2.4. In particular, we see that

$$\begin{aligned} & (\mu \mathbf{I} + 2\gamma \mathbf{\Omega} + 2\mathbf{X}^T \mathbf{X})^{-1} \\ &= \mathbf{M}^{-1} - 2\mathbf{M}^{-1} \mathbf{X}^T (\mathbf{I} + 2\mathbf{X} \mathbf{M}^{-1} \mathbf{X}^T)^{-1} \mathbf{X} \mathbf{M}^{-1}; \end{aligned}$$

computing this inverse only requires computing the inverse of \mathbf{M} and the inverse of the $n \times n$ matrix $\mathbf{I} + 2\mathbf{X} \mathbf{M}^{-1} \mathbf{X}^T$.

Next \mathbf{y} is updated by

$$\begin{aligned} \mathbf{y}^{t+1} &= \arg \min_{\mathbf{y} \in \mathbf{R}^p} L_\mu(\mathbf{x}^{t+1}, \mathbf{y}, \mathbf{z}^t) \\ &= \arg \min_{\mathbf{y}} \lambda \|\mathbf{y}\|_1 + \frac{\mu}{2} \|\mathbf{y} - \mathbf{x}^{t+1} - \mathbf{z}^t / \mu\|^2. \end{aligned}$$

Algorithm 6: Alternating direction method of multipliers for solving (5)

Data: Start with initial iterates $\mathbf{x}^0 = \mathbf{y}^0$ and step length μ .

Result: Solution $\beta^* = \mathbf{x}^* = \mathbf{y}^*$ of (5).

for $t = 0, 1, 2 \dots$ *until converged*

 Update \mathbf{x} by (20):

$$(\mu \mathbf{I} + \mathbf{A})\mathbf{x}^{t+1} = \mathbf{d} + \mu \mathbf{y}^t - \mathbf{z}^t ..$$

 Update \mathbf{y} using soft thresholding (21):

$$\mathbf{y}^{t+1} = S_\lambda(\mathbf{x}^{t+1} + \mathbf{z}^t / \mu)$$

 Update \mathbf{z} using approximate dual ascent (22):

$$\mathbf{z}^{t+1} = \mathbf{z}^t + \mu(\mathbf{x}^{t+1} - \mathbf{y}^{t+1})$$

end

That is, \mathbf{y}^{t+1} is updated as the value of the soft thresholding operator of the ℓ_1 -norm at $\mathbf{z}^t / \mu + \mathbf{x}^{t+1}$:

$$\mathbf{y}^{t+1} = S_\lambda(\mathbf{x}^{t+1} + \mathbf{z}^t / \mu). \quad (21)$$

Finally, the dual variable \mathbf{z} is updated using the approximate dual ascent step

$$\mathbf{z}^{t+1} = \mathbf{z}^t + \mu(\mathbf{x}^{t+1} - \mathbf{y}^{t+1}). \quad (22)$$

This approach is summarized in Algorithm 6. It is well-known that the ADMM generates a sequence of iterates which converge linearly to an optimal solution of (17) under certain strong convexity assumptions on f and g and rank assumptions on \mathbf{A} and \mathbf{B} , all of which are satisfied by our problem (19) when Ω is positive definite (see, for example, [Deng and Yin \[2012\]](#)). It follows that the sequence of iterates $\{\mathbf{x}^t, \mathbf{y}^t, \mathbf{z}^t\}$ generated by Algorithm 6 converges to a minimizer of $F(\beta)$; that is, $\mathbf{x}^t - \mathbf{y}^t \rightarrow \mathbf{0}$ and $F(\mathbf{x}^t), F(\mathbf{y}^t)$ converge linearly to the minimum value of F .

2.4 Computational Requirements

To motivate the use of our proposed proximal methods for the minimization of (5), we briefly sketch the per-iteration computational costs of each of our methods. We will see that for certain choices of regularization parameters, the number of floating point operations needed for each iteration scales linearly with the size of the data.

The most expensive step of both the proximal gradient method (Algorithm 3) and the accelerated proximal gradient method (Algorithm 4) is the evaluation

of the gradient ∇f . Given a vector $\beta \in \mathbf{R}^p$, the gradient at β is given by

$$\begin{aligned} \nabla f(\beta) &= \mathbf{A}\beta = 2 \left(\mathbf{X}^T \mathbf{X} + \gamma \Omega \right) \beta \\ &= 2\mathbf{X}^T \mathbf{X}\beta + 2\gamma \Omega \beta. \end{aligned}$$

The product $\mathbf{X}^T \mathbf{X}\beta$ can be computed using $\mathcal{O}(np)$ floating point operations by computing $\mathbf{y} = \mathbf{X}\beta$ and then $\mathbf{X}^T \mathbf{y}$. On the other hand, the product $\Omega \beta$ requires $\mathcal{O}(p^2)$ flops for unstructured Ω . However, if we use a *structured* regularization parameter Ω we can significantly decrease this computational cost. Consider the following examples:

- Suppose that Ω is a diagonal matrix: $\Omega = \text{Diag}(\mathbf{u})$ for some vector $\mathbf{u} \in \mathbf{R}_+^p$. Then the product $\Omega \beta$ can be computed using $\mathcal{O}(p)$ flops:

$$(\Omega \beta)_i = u_i \beta_i.$$

Moreover, we can estimate the Lipschitz constant $\|\mathbf{A}\|$ for use in choosing the step size α by

$$\|\mathbf{A}\| \leq 2\gamma \|\Omega\| + 2\|\mathbf{X}\|_F^2 = 2\gamma \|\mathbf{u}\|_\infty + 2\|\mathbf{X}\|_F^2,$$

which requires $\mathcal{O}(np)$ flops, primarily to compute the norm $\|\mathbf{X}\|_F^2$.

- If the use of diagonal Ω is inappropriate, we could store Ω in factored form $\Omega = \mathbf{R}\mathbf{R}^T$ where $\mathbf{R} \in \mathbf{R}^{p \times r}$, and r is the rank of Ω . In this case, we have

$$\Omega \beta = \mathbf{R}(\mathbf{R}^T \beta),$$

which can be computed at a cost of $\mathcal{O}(rp)$ flops. Thus, if we use a low-rank parameter Ω , say $r \leq \mathcal{O}(n)$, we can compute the gradient using $\mathcal{O}(np)$ flops. Similarly, we can estimate the step size α using

$$\|\mathbf{A}\| \leq 2\|\mathbf{R}\|_F^2 + 2\|\mathbf{X}\|_F^2$$

(computed at a cost of $\mathcal{O}(rp + np)$ flops).

In either case, using a diagonal Ω or low-rank factored Ω , each iteration of the proximal gradient method or the accelerated proximal gradient method requires $\mathcal{O}(np)$ flops. Similar improvements can be made if Ω is tridiagonal, banded, sparse, or otherwise nicely structured.

Similarly, the use of structured Ω can lead to significant improvements in computational efficiency in our ADMM algorithm. The main computational bottleneck of this method is the solution of the linear system in the update of \mathbf{x} :

$$(\mu \mathbf{I} + \mathbf{A})\mathbf{x}^{t+1} = \mathbf{d} + \mu \mathbf{y}^t - \mathbf{z}^t.$$

Without taking advantage of the structure of \mathbf{A} , we can solve this system using a Cholesky factorization preprocessing step (at a cost of $\mathcal{O}(p^3)$ flops) and substitution to solve the resulting triangular systems (at a cost of $\mathcal{O}(p^2)$ flops per-iteration). However, we can often use the Sherman-Morrison-Woodbury Lemma to solve this system more efficiently using the structure of \mathbf{A} . Indeed, fix t and let $\mathbf{b} = \mathbf{d} + \mu\mathbf{y}^t - \mathbf{z}^t$. Then we update \mathbf{x} by

$$\mathbf{x} = (\mu\mathbf{I} + \mathbf{A})^{-1}\mathbf{b}.$$

If $\mathbf{M} = \mu\mathbf{I} + 2\gamma\mathbf{\Omega}$ then we have

$$\begin{aligned} (\mu\mathbf{I} + \mathbf{A})^{-1} &= (\mu\mathbf{I} + 2\gamma\mathbf{\Omega} + 2\mathbf{X}^T\mathbf{X})^{-1} \\ &= (\mathbf{M} + 2\mathbf{X}^T\mathbf{X})^{-1} \\ &= \mathbf{M}^{-1} + 2\mathbf{M}^{-1}\mathbf{X}^T (\mathbf{I} + 2\mathbf{X}\mathbf{M}^{-1}\mathbf{X}^T)^{-1} \mathbf{X}^T\mathbf{M}^{-1}. \end{aligned}$$

The matrix $\mathbf{I} + 2\mathbf{X}\mathbf{M}^{-1}\mathbf{X}^T$ is $n \times n$, so we may solve any linear system with this coefficient matrix using $\mathcal{O}(n^3)$ flops; a further $\mathcal{O}(n^2p)$ flops are needed to compute the coefficient matrix if given \mathbf{M}^{-1} . Thus, the main computational burden of this update step is the inversion of the matrix \mathbf{M} . As before, we want to choose $\mathbf{\Omega}$ so that we can exploit its structure. Consider the following cases.

- If $\mathbf{\Omega} = \text{Diag}(\mathbf{u})$ is diagonal, then \mathbf{M} is also diagonal with

$$[\mathbf{M}^{-1}]_{ii} = \frac{1}{\mu + 2\gamma u_i}.$$

Thus, we require $\mathcal{O}(p)$ flops to compute $\mathbf{M}^{-1}\mathbf{v}$ for any vector $\mathbf{v} \in \mathbf{R}^p$.

- On the other hand, if $\mathbf{\Omega} = \mathbf{R}\mathbf{R}^T$, where $\mathbf{R} \in \mathbf{R}^{p \times r}$, then we may use the Sherman-Morrison-Woodbury identity to compute \mathbf{M}^{-1} :

$$\mathbf{M}^{-1} = \frac{1}{\mu}\mathbf{I} - \frac{2\gamma}{\mu^2}\mathbf{R} \left(\mathbf{I} + \frac{2\gamma}{\mu}\mathbf{R}^T\mathbf{R} \right)^{-1} \mathbf{R}^T.$$

Therefore, we can solve any linear system with coefficient matrix \mathbf{M} at a cost of $\mathcal{O}(r^2p)$ flops (for the formation and solution of the system with coefficient matrix $\mathbf{I} + \frac{2\gamma}{\mu}\mathbf{R}^T\mathbf{R}$).

In either case, we never actually compute the matrices \mathbf{M}^{-1} and $(\mu\mathbf{I} + \mathbf{A})^{-1}$ explicitly. Instead, we update \mathbf{x} as the solution of a sequence of linear systems and matrix-vector multiplications, at a total cost of $\mathcal{O}(n^2p)$ flops (in the diagonal case) or $\mathcal{O}((r^2 + n^2)p)$ flops (in the factored case). Thus, if the number

Prox Grad	∇f	$\ \mathbf{A}\ $
Diagonal	$\mathcal{O}(np)$	$\mathcal{O}(np)$
Rank r	$\mathcal{O}(rp + np)$	$\mathcal{O}(rp + np)$
Full rank	$\mathcal{O}(p^2)$	$\mathcal{O}(p^2 \log p)$
<hr/>		
ADMM	$(\mu\mathbf{I} + \mathbf{A})\mathbf{x} = \mathbf{b}$	
Diagonal	$\mathcal{O}(n^3 + n^2p)$	
Rank r	$\mathcal{O}(n^3 + n^2p + r^2p)$	
Full rank	$\mathcal{O}(p^3)$	

Table 1: Upper bounds on floating point operation counts for most time consuming steps of each algorithm. For our (accelerated) proximal gradient method, these are the matrix-vector multiplication to compute the gradient ∇f and the estimation of the Lipschitz constant using $\|\mathbf{A}\| \leq 2(\|\mathbf{\Omega}\| + \|\mathbf{X}\|_F^2)$ to define the step length; for ADMM, this is the solution of the linear system in the update of \mathbf{x} .

of observations n is much smaller than the number of features p , then the per-iteration computation scales roughly linearly with p . Table 2.4 summarizes these estimates of per-iteration computational costs for each proposed algorithm. Further, we should note that these bounds on per-iteration cost assume that the iterates $\boldsymbol{\beta}$ and \mathbf{x} are dense; the soft-thresholding step of the proximal gradient algorithm typically induces $\boldsymbol{\beta}$ containing many zeros, suggesting that further improvements can be made by using sparse arithmetic.

2.5 Convergence of our block coordinate descent method

In this section, we investigate the convergence properties of our block coordinate descent method (Algorithm 1). Our two main results, Theorem 2.4 and Theorem 2.5, are specializations of standard results for alternating minimization algorithms; we include these results and their proofs for completeness.

We first note that the Lagrangian $L : \mathbf{R}^K \times \mathbf{R}^p \times \mathbf{R} \times \mathbf{R}^{k-1} \rightarrow \mathbf{R}$ of (2) is given by

$$\begin{aligned} L(\boldsymbol{\theta}, \boldsymbol{\beta}, \psi, \mathbf{v}) &= \|\mathbf{Y}\boldsymbol{\theta} - \mathbf{X}\boldsymbol{\beta}\|^2 + \gamma\boldsymbol{\beta}^T\mathbf{\Omega}\boldsymbol{\beta} + \lambda\|\boldsymbol{\beta}\|_1 \\ &\quad + \psi(\boldsymbol{\theta}^T\mathbf{Y}^T\mathbf{Y}\boldsymbol{\theta} - n) + \mathbf{v}^T\mathbf{U}\boldsymbol{\theta}, \end{aligned} \quad (23)$$

where $\mathbf{U}^T = (\mathbf{Y}^T\mathbf{Y}\boldsymbol{\theta}_1, \mathbf{Y}^T\mathbf{Y}\boldsymbol{\theta}_2, \dots, \mathbf{Y}^T\mathbf{Y}\boldsymbol{\theta}_{k-1})$. Note that the Lagrangian is *not* a convex function in general. However, L is the sum of the (possibly) non-convex quadratic $\|\mathbf{Y}\boldsymbol{\theta} - \mathbf{X}\boldsymbol{\beta}\|^2 + \psi(\boldsymbol{\theta}^T\mathbf{Y}^T\mathbf{Y}\boldsymbol{\theta} - n) + \gamma\boldsymbol{\beta}^T\mathbf{\Omega}\boldsymbol{\beta} + \mathbf{v}^T\mathbf{U}\boldsymbol{\theta}$ and the convex nonsmooth function $\lambda\|\boldsymbol{\beta}\|_1$; therefore, L is subdifferentiable, with subdifferential at $(\boldsymbol{\beta}, \boldsymbol{\theta})$ given by the sum of the gradient of

the smooth term at $(\boldsymbol{\beta}, \boldsymbol{\theta})$ and the subdifferential of the convex nonsmooth term at $(\boldsymbol{\beta}, \boldsymbol{\theta})$.

We now provide our first convergence result, specifically, that Algorithm 1 generates a convergent sequence of function values.

Theorem 2.4 *Suppose that the sequence of iterates $\{(\boldsymbol{\theta}^t, \boldsymbol{\beta}^t)\}_{t=0}^\infty$ is generated by Algorithm 1. Then the corresponding sequence of objective function values $\{F(\boldsymbol{\theta}^t, \boldsymbol{\beta}^t)\}_{t=0}^\infty$ defined by*

$$F(\boldsymbol{\theta}, \boldsymbol{\beta}) := \|\mathbf{Y}\boldsymbol{\theta} - \mathbf{X}\boldsymbol{\beta}\|^2 + \gamma\boldsymbol{\beta}^T\boldsymbol{\Omega}\boldsymbol{\beta} + \lambda\|\boldsymbol{\beta}\|_1$$

is convergent.

Proof: Suppose that, after t iterations, we have iterates $(\boldsymbol{\theta}^t, \boldsymbol{\beta}^t)$ with objective function value $F(\boldsymbol{\theta}^t, \boldsymbol{\beta}^t)$. Recall that we obtain $\boldsymbol{\beta}^{t+1}$ as the solution of (5). Moreover, note that $\boldsymbol{\beta}^t$ is also feasible for (5). This immediately implies that

$$F(\boldsymbol{\theta}^t, \boldsymbol{\beta}^t) \geq F(\boldsymbol{\theta}^t, \boldsymbol{\beta}^{t+1}).$$

On the other hand, $\boldsymbol{\theta}^{t+1}$ is the solution of (3) with $\boldsymbol{\beta} = \boldsymbol{\beta}^{t+1}$. Therefore, we have

$$F(\boldsymbol{\theta}^t, \boldsymbol{\beta}^t) \geq F(\boldsymbol{\theta}^t, \boldsymbol{\beta}^{t+1}) \geq F(\boldsymbol{\theta}^{t+1}, \boldsymbol{\beta}^{t+1}).$$

It follows that the sequence of function values $\{F(\boldsymbol{\theta}^t, \boldsymbol{\beta}^t)\}_{t=1}^\infty$ is nonincreasing. Moreover, the objective function $F(\boldsymbol{\theta}, \boldsymbol{\beta})$ is nonnegative for all $\boldsymbol{\theta}$ and $\boldsymbol{\beta}$. Therefore, $\{F(\boldsymbol{\theta}^t, \boldsymbol{\beta}^t)\}_{t=1}^\infty$ is convergent as a monotonic bounded sequence. ■

We also have the following theorem, which establishes that every convergent subsequence of $\{(\boldsymbol{\theta}^t, \boldsymbol{\beta}^t)\}_{t=1}^\infty$ converges to a stationary point of (2).

Theorem 2.5 *Let $\{(\boldsymbol{\theta}^t, \boldsymbol{\beta}^t)\}_{t=1}^\infty$ be the sequence of points generated by Algorithm 1. Suppose that $\{(\boldsymbol{\theta}^{t_j}, \boldsymbol{\beta}^{t_j})\}_{j=1}^\infty$ is a convergent subsequence of $\{(\boldsymbol{\theta}^t, \boldsymbol{\beta}^t)\}_{t=1}^\infty$ with limit $(\boldsymbol{\theta}^*, \boldsymbol{\beta}^*)$. Then $(\boldsymbol{\theta}^*, \boldsymbol{\beta}^*)$ is a stationary point of (2): $(\boldsymbol{\theta}^*, \boldsymbol{\beta}^*)$ is feasible for (2) and there exists $\psi^* \in \mathbf{R}$ and $\mathbf{v}^* \in \mathbf{R}^{k-1}$ such that*

$$\mathbf{0} \in \partial L(\boldsymbol{\theta}^*, \boldsymbol{\beta}^*, \psi^*, \mathbf{v}^*),$$

where $\partial L(\boldsymbol{\theta}, \boldsymbol{\beta}, \psi, \mathbf{v})$ denotes the subdifferential of the Lagrangian function L with respect to the primal variables $(\boldsymbol{\theta}, \boldsymbol{\beta})$.

To prove Theorem 2.5, we first establish the following lemma, which establishes that the limit point $(\boldsymbol{\theta}^*, \boldsymbol{\beta}^*)$ minimizes F with respect to each primal variable with the other fixed; that is, $\boldsymbol{\theta}^*$ minimizes $F(\cdot, \boldsymbol{\beta}^*)$ and $\boldsymbol{\beta}^*$ minimizes $F(\boldsymbol{\theta}^*, \cdot)$.

Lemma 2.2 *Let $\{(\boldsymbol{\theta}^t, \boldsymbol{\beta}^t)\}_{t=1}^\infty$ be the sequence of points generated by Algorithm 1. Suppose that $\{(\boldsymbol{\theta}^{t_j}, \boldsymbol{\beta}^{t_j})\}_{j=1}^\infty$ is a convergent subsequence of $\{(\boldsymbol{\theta}^t, \boldsymbol{\beta}^t)\}_{t=1}^\infty$ with limit $(\boldsymbol{\theta}^*, \boldsymbol{\beta}^*)$. Then*

$$F(\boldsymbol{\theta}, \boldsymbol{\beta}^*) \geq F(\boldsymbol{\theta}^*, \boldsymbol{\beta}^*) \quad (24)$$

$$F(\boldsymbol{\theta}^*, \boldsymbol{\beta}) \geq F(\boldsymbol{\theta}^*, \boldsymbol{\beta}^*) \quad (25)$$

for all feasible $\boldsymbol{\theta} \in \mathbf{R}^k$ and $\boldsymbol{\beta} \in \mathbf{R}^p$.

Proof: We first establish (25). Consider $(\boldsymbol{\theta}^{t_j}, \boldsymbol{\beta}^{t_j})$. By our update step for $\boldsymbol{\beta}$, we note that

$$\boldsymbol{\beta}^{t_j} = \arg \min_{\boldsymbol{\beta} \in \mathbf{R}^p} F(\boldsymbol{\theta}^{t_j}, \boldsymbol{\beta}).$$

Thus, for all $j = 1, 2, \dots$, we have $F(\boldsymbol{\theta}^{t_j}, \boldsymbol{\beta}) \geq F(\boldsymbol{\theta}^{t_j}, \boldsymbol{\beta}^{t_j})$ for all $\boldsymbol{\beta} \in \mathbf{R}^p$. Taking the limit as $j \rightarrow \infty$ and using the continuity of F establishes (25).

Next, note that, for every $j = 1, 2, \dots$, we have

$$\begin{aligned} \boldsymbol{\theta}^{t_j+1} &= \arg \min_{\boldsymbol{\theta} \in \mathbf{R}^k} F(\boldsymbol{\theta}, \boldsymbol{\beta}^{t_j}) \\ \text{s.t.} \quad &\boldsymbol{\theta}^T \mathbf{Y}^T \mathbf{Y} \boldsymbol{\theta} = n \\ &\boldsymbol{\theta}^T \mathbf{Y}^T \mathbf{Y} \boldsymbol{\theta}_\ell = 0 \quad \forall \ell < k. \end{aligned}$$

This implies that

$$\begin{aligned} F(\boldsymbol{\theta}, \boldsymbol{\beta}^{t_j}) &\geq F(\boldsymbol{\theta}^{t_j+1}, \boldsymbol{\beta}^{t_j}) \\ &\geq F(\boldsymbol{\theta}^{t_j+1}, \boldsymbol{\beta}^{t_j+1}) \\ &\geq F(\boldsymbol{\theta}^{t_j+1}, \boldsymbol{\beta}^{t_j+1}) \end{aligned}$$

by the monotonicity of the sequence of function values and the fact that $t_j < t_j + 1 \leq t_{j+1}$. Taking the limit as $j \rightarrow \infty$ and using the continuity of F establishes (24). This completes the proof. ■

We are now ready to prove Theorem 2.5.

Proof: (of Theorem 2.5). The form of the subdifferential of L implies that $(\mathbf{g}_\theta, \mathbf{g}_\beta) \in \partial L(\boldsymbol{\theta}, \boldsymbol{\beta}, \psi, \mathbf{v})$ if and only if

$$\mathbf{g}_\theta = 2(1 + \psi)\mathbf{Y}^T \mathbf{Y} \boldsymbol{\theta} - 2\mathbf{Y}^T \mathbf{X} \boldsymbol{\beta} + \mathbf{U}^T \mathbf{v} \quad (26)$$

$$\mathbf{g}_\beta \in 2(\mathbf{X}^T \mathbf{X} + \gamma\boldsymbol{\Omega})\boldsymbol{\beta} - 2\mathbf{X}^T \mathbf{Y} \boldsymbol{\theta} + \lambda\partial\|\boldsymbol{\beta}\|_1 \quad (27)$$

for all $\mathbf{v} \in \mathbf{R}^{k-1}$ and $\psi \in \mathbf{R}$. Equation (25) implies that $\boldsymbol{\beta}^* = \arg \min_{\boldsymbol{\beta} \in \mathbf{R}^p} F(\boldsymbol{\theta}^*, \boldsymbol{\beta})$. Thus, by the first order necessary conditions for unconstrained convex optimization, we must have

$$\begin{aligned} \mathbf{0} &\in \partial \left(\frac{1}{2}(\boldsymbol{\beta}^*)^T \mathbf{A} \boldsymbol{\beta}^* + \mathbf{d}^T \boldsymbol{\beta}^* + \lambda\|\boldsymbol{\beta}^*\|_1 \right) \\ &= 2(\mathbf{X}^T \mathbf{X} + \gamma\boldsymbol{\Omega})\boldsymbol{\beta}^* - 2\mathbf{X}^T \mathbf{Y} \boldsymbol{\theta}^* + \lambda\partial\|\boldsymbol{\beta}^*\|_1; \end{aligned} \quad (28)$$

here $\partial\|\beta\|_1$ denotes the subdifferential of the ℓ_1 -norm at the point β .

On the other hand, (24) implies

$$\begin{aligned} \theta^* &= \arg \min_{\theta \in \mathbf{R}^K} \|\mathbf{Y}\theta - \mathbf{X}\beta^*\|^2 \\ \text{s.t.} \quad & \theta^T \mathbf{Y}^T \mathbf{Y} \theta = n, \\ & 2\theta^T \mathbf{Y}^T \mathbf{Y} \theta_\ell = 0, \quad \forall \ell < k. \end{aligned} \quad (29)$$

Moreover, the problem (29) satisfies the linear independence constraint qualification. Indeed, the set of active constraint gradients $\{2\mathbf{Y}^T \mathbf{Y} \theta, 2\mathbf{Y}^T \mathbf{Y} \theta_1, \dots, 2\mathbf{Y}^T \mathbf{Y} \theta_{k-1}\}$ is linearly independent for any feasible $\theta \in \mathbf{R}^K$ by the $\mathbf{Y}^T \mathbf{Y}$ -conjugacy of $\{\theta, \theta_1, \dots, \theta_{k-1}\}$. Therefore, there exist Lagrange multipliers ψ^*, \mathbf{v}^* such that

$$\mathbf{0} = 2(1 + \psi^*)\mathbf{Y}^T \mathbf{Y} \theta^* - 2\mathbf{Y}^T \mathbf{X} \beta^* + \mathbf{U}^T \mathbf{v}^* \quad (30)$$

by the first-order necessary conditions for optimality (see Nocedal and Wright [2006, Theorem 12.1]). We see that $\mathbf{0} \in \partial L(\theta^*, \beta^*, \psi^*, \mathbf{v}^*)$ by combining (28) and (30). This completes the proof. \blacksquare

3 Numerical Simulations

We next compare the performance of our proposed approaches with standard methods for penalized discriminant analysis in several numerical experiments. In particular, we compare the implementations of the block coordinate descent method Algorithm 1 where each discriminant direction β is updated using the proximal gradient method given by Algorithm 3 (SDAP), the accelerated proximal method given by Algorithm 4 (SDAAP), and the alternating direction method of multipliers given by Algorithm 6 (SDAD), with the Sparse Zero Variance Discriminant Analysis (SZVD) method proposed in Ames and Hong [2016], and the algorithm for solving the sparse optimal scoring problem proposed in Clemmensen et al. [2011]. All simulations were conducted using R version 3.2.3 and our heuristics are implemented in R as the package **accSDA**³. The runs on the benchmarking data sets were performed on a laptop with an i7-8700K processor clocked at 3.70GHz. The runs on the synthetic data sets were performed on a cluster where each node had an Intel Xeon E5-2660 v2 CPU clocked at 2.20GHz.

3.1 Classification of Spectral and Time Series Data

We first apply each of these methods to learn classification rules for the following data sets: the *Penicillium*

³Available at <https://github.com/gumeo/accSDA> and <https://cran.r-project.org/web/packages/accSDA>

data set from [Clemmensen et al., 2007] of multi-spectral images of three *Penicillium* species that are almost visually indistinguishable ($p = 3542, K = 3, n = 36$, training sample size = 24, testing sample size = 12); *Electrocardiogram measurements (ECG)* of a 67-year old male taken on two dates, five days apart, before and after corrective cardiac surgery ($p = 136, K = 2, n = 884$, training size = 23, testing size = 861); food spectrogram observations of either Arabica or Robusta variants of instant coffee ($p = 286, K = 2, n = 56$, training size = 28, testing size = 28); food spectrogram observations of extra virgin olive oil originating from one of four countries ($p = 570, K = 4, n = 60$, training size = 30, testing size = 30). The final three data sets were obtained from the UC Riverside time series classification repository [Keogh et al., 2006]. We use each heuristic to obtain $q = K - 1$ sparse discriminant vectors and then perform nearest-centroid classification after projection onto the subspace spanned by these discriminant directions. The results of our experiments are summarized in Table 2.

The sparse discriminant analysis heuristics SDAP, SDAAP, SDAD, and SDA require training of the regularization parameters γ , $\mathbf{\Omega}$, and λ . In all experiments, we set $\gamma = 10^{-3}$ and $\mathbf{\Omega}$ to be the $p \times p$ identity matrix $\mathbf{\Omega} = \mathbf{I}$. We train the remaining parameter λ using N -fold cross validation. Specifically, we choose λ from a set of potential λ of the form $\bar{\lambda}/2^c$ for $c = 9, 8, 7, \dots, -1, -2, -3$ and $\bar{\lambda}$ chosen so that the problem has nontrivial solution for all considered λ . Note that (10) has optimal solution given by $\beta^* = \mathbf{A}^{-1} \mathbf{d}$ if we set $\lambda = 0$; this implies that choosing

$$\bar{\lambda} = \frac{(\beta^*)^T \mathbf{d} - \frac{1}{2}(\beta^*)^T \mathbf{A} \beta^*}{\|\beta^*\|_1}$$

ensures that there exists at least one solution β^* with value strictly less than zero. We pick as our regularization parameter the value of λ with fewest average number of misclassification errors over training-validation splits amongst all λ which yield discriminant vectors containing at most 15% nonzero entries. We set the number of folds $N = 5, 5, 7, 15$ for Pen, ECG, Coffee, and Olive oil data sets respectively. We terminate each proximal algorithm in the inner loop after 1000 iterations or a 10^{-5} suboptimal solution is obtained; the outer block coordinate descent loop is stopped after a maximum number of 250 iterations or a 10^{-3} suboptimal solution has been found. The augmented Lagrangian parameter $\mu = 2.5$ was used in all experiments in the ADMM method (SDAD). The backtracking versions of SDAP and SDAAP use the value of $\bar{L} = 0.25$ for the initial estimate of the

Time Series	Measures	SDAP	SDAAP	SDAD	SDAPbt	SDAAPbt	SDA
Pen	numErr	0	0	0	0	0	0
$p = 3542$	fracErr	0	0	0	0	0	0
$K = 3$	feats	688	365	57	1242	1106	109
$n_{train} = 24$	fracFeats	0.10	0.05	0.01	0.18	0.16	0.02
$n_{test} = 12$	time	1386.23	23.37	152.61	1477.16	181.15	610.35
ECG	numErr	23	86	79	25	85	42
$p = 136$	fracErr	0.3	0.10	0.09	0.03	0.10	0.05
$K = 2$	feats	20	11	22	12	16	16
$n_{train} = 23$	fracFeats	0.15	0.08	0.16	0.09	0.12	0.12
$n_{test} = 861$	time	11.26	4.04	10.37	26.7	12.48	0.98
Coffee	numErr	0	0	0	0	0	0
$p = 286$	fracErr	0	0	0	0	0	0
$K = 2$	feats	22	20	43	34	36	4
$n_{train} = 28$	fracFeats	0.08	0.07	0.15	0.12	0.13	0.01
$n_{test} = 28$	time	36.47	5.82	24.59	46.21	19.76	2.47
OliveOil	numErr	3	5	2	2	5	3
$p = 570$	fracErr	0.1	0.17	0.07	0.07	0.17	0.10
$K = 4$	feats	60	26	122	73	60	60
$n_{train} = 30$	fracFeats	0.04	0.02	0.07	0.04	0.04	0.04
$n_{test} = 30$	time	230.48	54.41	173.66	455.69	188.12	185.40

Table 2: Comparison of classification performance of benchmarking data. Each block reports the number of classification errors on out-of-sample testing observations (numErr), fraction of classification errors (fracErr), number of nonzero features used for classification (feats), fraction of nonzero features (fracFeat), and time (in seconds) needed to train the discriminant vectors (time).

Lipschitz constant and $\eta = 1.25$ for the scalar multiplier.

We train any regularization parameters in SZVD using a similar procedure. In particular, we set the maximum value of the regularization parameter γ to be $\hat{\beta}^T \mathbf{B} \hat{\beta} / \|\hat{\beta}\|_1$, where $\hat{\beta}$ is the optimal solution of the unpenalized SZVD problem and \mathbf{B} is the sample between-class covariance matrix of the training data, and choose γ from an exponentially spaced grid using N -fold cross-validation; this approach is consistent with that in [Ames and Hong, 2016]. The number of folds N for each data set was identical to that in the SDA cross validation scheme described above. We select the value of γ which minimizes misclassification error amongst all sets of discriminant vectors with at most 35% nonzero entries; this acceptable sparsity threshold is chosen to be higher than that in the SDA experiments, due to the tendency of SZVD to misconverge to the trivial all-zero solution for large values of γ . We stop SZVD after a maximum of 1000 iterations or a solution satisfying the stopping tolerance of 10^{-5} is obtained. We use the augmented Lagrangian penalty parameter $\beta = 2.5$ in SZVD in all experiments.

3.2 Gaussian data

We performed similar simulations investigating efficacy of our heuristics for classification of Gaussian data. In each experiment, we generate data consisting of p -dimensional vectors from one of K multivariate Normal distributions. Specifically, we obtain training observations corresponding to the i th class, $i = 1, 2, \dots, K$, by sampling 25 observations from the multivariate Normal distribution with mean $\boldsymbol{\mu}_i \in \mathbf{R}^p$ with entries indexed by $100(i-1), \dots, 100i$ equal to 0.7 and all remaining entries equal to 0, and covariance matrix $\boldsymbol{\Sigma} \in \mathbf{R}^{p \times p}$ constructed as follows.

- *Type 1 data:* in the first set of simulations, all features are correlated with $\Sigma_{ij} = r$ for all $i \neq j$ and $\Sigma_{ii} = 1$ for all i . We conduct the experiment for all $K \in \{2, 4\}, r \in \{0, 0.1, 0.5, 0.9\}$.
- *Type 2 data:* in the second set of simulations, $\boldsymbol{\Sigma}$ is a block diagonal matrix with 100×100 blocks. For each pair of indices (i, j) in the same block we set $\Sigma_{ij} = r^{|i-j|}$, and set $\Sigma_{ij} = 0$ otherwise. As before, we repeat the experiment for each $K \in \{2, 4\}, r \in \{0, 0.1, 0.5, 0.9\}$.

For each experiment, we sample 250 testing observations from each class in the same manner as the training data.

For each (K, r) pair we generate 20 data sets and use nearest centroid classification following projection onto the span of the discriminant directions to test the five LDA heuristics SDA, SDAP, SDAAP, SDAD, and SZVD. All input parameters are defined as in Section 3.1. We train any regularization parameters in the same fashion as in Section 3.1 using N -fold cross validation; we set a maximum fraction of nonzero features to 0.3 in the cross validation scheme. Tables 3, 4, 5, and 6 summarize the results of these experiments.

3.3 Multispectral X-ray images and Ω of varying rank

To demonstrate empirically the improvement in runtime obtained by using a low-rank Ω in the elastic-net penalty, we perform pixelwise classification on multispectral X-ray images, like presented in [Einarsson et al., 2017]. The multispectral X-ray images are scans of food items, where each pixel contains 128 measurements (channels) corresponding to attenuation of X-rays emitted at different wavelengths (See Fig. 1). The measurements in each pixel thus give us a profile for the material positioned at that pixel’s location (See Fig. 2).

We start by preprocessing the scans similar to [Einarsson et al., 2017] in order to remove scanning artifacts and normalize the intensities between scans. We scale the measurements in each pixel by the 95% quantile of the corresponding 128 measurements instead of the maximum. This scaling approach is more robust in the sense that it is less sensitive to outliers compared to using the maximum.

We create our training data by manually selecting rectangular patches from six scans. We have three classes, namely *background*, *minced meat* and *foreign objects*. We further subsample the observations to have balanced number of observations, where the class *foreign objects* was under represented. In the end we have 521 observations per class, where each observation corresponds to a single pixel. This data was used to generate Fig. 2. For training we use 100 samples per class, and the rest is allocated to a final test set.

This process yields 128 variables per observation, but in order to get more spatially consisted classification, we also include data from the pixels located above, to the right, below and to the left of the observed pixel. Thus we have $p = 5 \cdot 128 = 640$ variables per observation. The measurements corre-

sponding to our observation are thus indexed according to spatial and spectral position, i.e., observation \mathbf{x}_i has measurements x_{ijk} , where $j \in \{0, 1, 2, 3, 4\}$ indicates which pixel the measurement belongs to (*center, above, right, bottom, left*), and $k \in \{1, 2, \dots, 128\}$ indicates which channel.

We can impose priors according to these relationships of the measurements in the Ω regularization matrix. We assume that the errors should vary smoothly in space and thus impose a Matérn covariance structure on Ω^{-1} [Matérn, 2013]:

$$C_\nu(d) = \sigma^2 \frac{2^{1-\nu}}{\Gamma(\nu)} \left(\sqrt{2\nu} \frac{d}{\rho} \right)^\nu K_\nu \left(\sqrt{2\nu} \frac{d}{\rho} \right). \quad (31)$$

The Matérn covariance structure (31) is governed by the distance d between measurements. In (31), Γ refers to the gamma function and K_ν is the modified Bessel function of the second kind. For this example we assume that all parameters are 1, except that ν is 0.5. We further assume that the distance between measurements x_{ijk} and $x_{ij'k'}$ from observation i is the Euclidean distance between the points (x_j, y_j, z_k) and $(x_{j'}, y_{j'}, z_{k'})$, where $x_j, y_j, x_{j'}, y_{j'} \in \{-1, 0, 1\}$ and $z_k, z_{k'} \in \{1, 2, \dots, 128\}$. The distance is thus the same as in the image grid (center, top, bottom, left, right pixel location), and z -dimension corresponds to the channel.

We use a stopping tolerance of 10^{-5} and a maximum of 1000 iterations for the inner loop using the accelerated proximal algorithm, and a stopping tolerance of 10^{-4} and maximum 1000 iterations for the outer block-coordinate loop. The regularization parameter for the l_1 -norm is selected as $\lambda = 10^{-3}$ and $\gamma = 10^{-1}$ for the Tikhonov regularizer. We present the run-time for varying r in Fig. 3 and the accuracy with respect to varying r in Fig. 4. There is a clear linear trend in rank r for the increase in runtime; this agrees with the analysis of Section 2.4. We also estimate the accuracy for a identity regularization matrix, i.e., $\Omega = \mathbf{I}$, with the same regularization parameters γ and λ and achieve accuracy of 0.948, which is approximately the same accuracy as when using Ω^{400} . To demonstrate the effect that the rank of Ω has on computational complexity, we obtain the singular value decomposition of $\Omega = \sum_{i=1}^p \sigma_i \mathbf{u}_i \mathbf{v}_i^T$, and construct a low-rank approximation to Ω using the first r singular vectors and singular values: $\Omega^r = \sum_{i=1}^r \sigma_i \mathbf{u}_i \mathbf{v}_i^T$. We supplied the same parameters to the function `sda` from the library `sparseLDA`; `sda` required 267 seconds to run and achieved an accuracy of 0.949. The maximum accuracy is achieved with the full regularization matrix, which is 0.957.

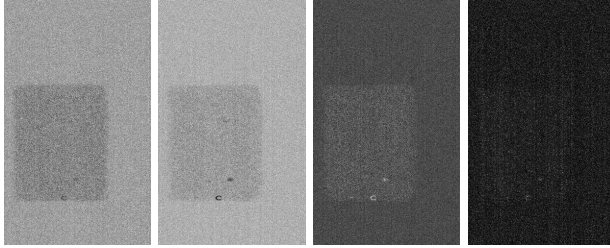


Figure 1: Grayscale images of different channels from a minced meat sample generated with a multispectral X-ray scanner after all preprocessing. From left to right are channels 2, 20, 50 and 100. The contrast decreases the higher we go in the channels and the variation in the measurements increases. Some foreign objects can be seen as small black dots.

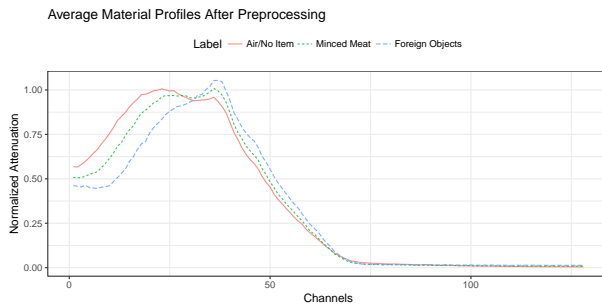


Figure 2: Profiles of materials seen in Fig. 1 over the 128 channels. The profile for each type of material, displayed here, is averaged over 500 pixels.

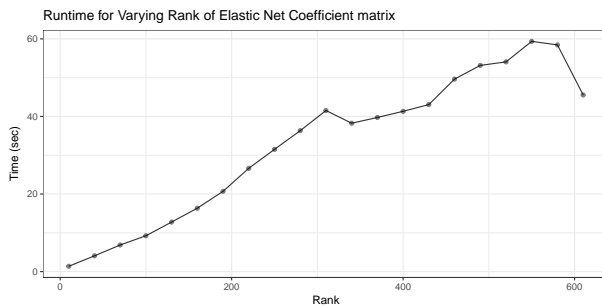


Figure 3: Running time when the rank of the elastic net coefficient matrix Ω is varied using Accelerated Proximal Gradient. The running time also includes the creation of the low-rank approximated Ω matrix.

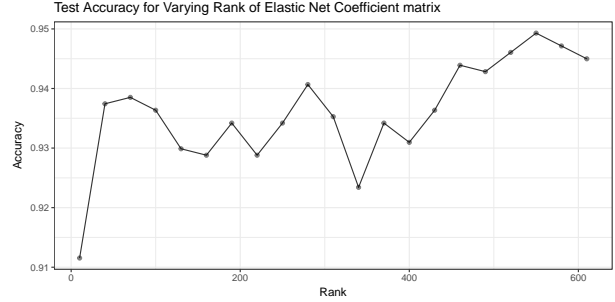


Figure 4: Test accuracy when the rank of the elastic net coefficient matrix Ω is varied using Accelerated Proximal Gradient.

3.4 Commentary

Our proximal methods for sparse discriminant analysis provide an improvement over the existing SDA approach in terms of classification error in almost all experiments, while we see a significant improvement in terms of computational resources used by the accelerated proximal gradient method (SDAAP) and ADMM (SDAD) over SDA. This improvement in run-time is most significant when applied to the Penicillium and synthetic data sets. This is not a coincidence. The per-iteration complexity of these methods is on the order of $\mathcal{O}(p)$ floating point operations per-iteration, compared to $\mathcal{O}(p^3)$ of the classical SDA method. We see this improvement is most significant when p is large, as it is for the Penicillium data set, where the per-iteration cost of $\mathcal{O}(p^3)$ flops is prohibitive. This improvement is not observed as acutely when p is small; in fact, SDA exhibits the shortest run-times for both the ECG and Coffee data sets, where p is the smallest. It is important to note that the slow convergence of the proximal gradient method (SDAP) without acceleration yields significantly longer run-times despite the improved per-iteration cost. We should also note that our use of cross validation causes significant variation in the performance of our heuristics for the ECG data set. This is because the trained discriminant vectors are sensitive to the split in the validation process, as the training set can become unbalanced.

4 Conclusion

We have proposed new algorithms for solving the sparse optimal scoring problem for high-dimensional linear discriminant analysis based on block coordinate descent and proximal operator evaluations. We observe that these algorithms provide significant improvement over existing approaches for solving the

SOS problem in terms of efficiency and scalability. These improvements are most acute in the case that specially structured Tikhonov regularization is employed in the SOS formulation; for example, the computational resources required for each iteration scales linearly with the dimension of the data if either a diagonal or low-rank matrix is used. Moreover, we establish that any convergent subsequence of iterates generated by one of our algorithms converges to a stationary point. Finally, numerical simulation establishes that our approach provides an improvement over existing methods for sparse discriminant analysis in terms of both quality of solution and run-time.

These results present several exciting avenues for future research. Although we focus primarily on the solution of the optimal scoring problem under regularization in the form of a generalized elastic net penalty, our approach should translate immediately to formulations with any nonsmooth convex penalty function. That is, the framework provided by Algorithm 1 can be applied to solve the SOS problem (2) obtained by applying an arbitrary convex penalty to the objective of the optimal scoring problem (1). The resulting optimization problem can be approximately solved by alternately minimizing with respect to the score vector θ using the formula (4) and with respect to the discriminant vector β by solving a modified version of (5). The proximal methods outlined in this paper can be applied to minimize with respect to β if the regularization function is convex, however it is unlikely that the computational resources necessary for this minimization will scale as favorably as with the generalized elastic net penalty. On the other hand, the convergence analysis presented in Section 2.5 extends immediately to this more general regularization framework. Of particular interest is the modification of this approach to provide means of learning discriminant vectors for data containing ordinal labels, data containing corrupted or missing observations, and semi-supervised settings.

Finally, the results found in Section 2.5 provide compelling evidence that any convergent subsequent of iterates generated by our block coordinate descent approach must converge to a stationary point. However, it is still unclear what conditions ensure that the sequence of iterates is convergent, or at what rate these subsequences converge; further study is required to better understand the convergence properties of these algorithms. Similarly, despite the empirical evidence provided in Section 3, it is unknown what conditions ensure that data is classifiable or when data can have its dimension reduced using sparse optimal scoring and, more generally, linear discriminant analysis. Extensive consistency analysis is needed to

determine theoretical classification error rates for distinguishing random variables drawn from distinct distributions.

4.1 Acknowledgements

We are grateful to Mingyi Hong for his helpful comments and suggestions. B. Ames was supported in part by University of Alabama Research Grant RG14678. G. Einarsson's PhD scholarship is funded by the Lundbeck foundation and the Technical University of Denmark. S. Atkins was part of the University Scholars Program at the University of Alabama while this research was conducted.

Appendix A. Proof of Lemma 2.1

To begin, we note that (3) has trivial solution $\theta = e$ for every $\beta = \beta^t \in \mathbf{R}^p$. Indeed, $\mathbf{Y}e = e$ by the structure of the indicator matrix \mathbf{Y} and $\sum_{i=1}^n x_{ij} = 0$ for all $j = 1, 2, \dots, p$ because our data has been centered to have sample mean equal to $\mathbf{0}$. This implies that (3) has the hidden constraint $\theta^T \mathbf{Y}^T \mathbf{Y} e = 0$. Therefore, we may reformulate (3) as

$$\begin{aligned} \min_{\theta \in \mathbf{R}^k} \quad & \|\mathbf{Y}\theta - \mathbf{X}\beta\|^2 \\ \text{s.t.} \quad & \theta^T \mathbf{Y}^T \mathbf{Y} \theta = n, \\ & \theta^T \mathbf{Y}^T \mathbf{Y} e = 0, \\ & \theta^T \mathbf{Y}^T \mathbf{Y} \theta_\ell = 0 \quad \ell < k. \end{aligned} \quad (32)$$

We wish to show that (32) has optimal solution $\hat{\theta}$ given by

$$\hat{\theta} = \frac{\mathbf{w}}{\sqrt{\mathbf{w}^T \mathbf{D} \mathbf{w}}}, \quad (33)$$

where $\mathbf{w} = (\mathbf{I} - \mathbf{Q}_k \mathbf{Q}_k^T \mathbf{D}) \mathbf{D}^{-1} \mathbf{Y}^T \mathbf{X} \beta$.

To do so, note that (32) satisfies the linear independence constraint qualification because the constraint gradients $\{2\mathbf{Y}^T \mathbf{Y} \theta, \mathbf{Y}^T \mathbf{Y} e, \mathbf{Y}^T \mathbf{Y} \theta_1, \dots, \mathbf{Y}^T \mathbf{Y} \theta_{k-1}\}$ are linearly independent. Moreover, the optimal value of (32) is bounded below by 0. Therefore, (32) has global minimizer, $\hat{\theta}$, which must satisfy the Karush-Kuhn-Tucker conditions, i.e., there exists $\mathbf{v} \in \mathbf{R}^k$, $\psi \in \mathbf{R}$ such that

$$\mathbf{Y}^T \mathbf{Y} \hat{\theta} - \mathbf{Y}^T \mathbf{X} \beta + \psi \mathbf{Y}^T \mathbf{Y} \hat{\theta} + \mathbf{Y}^T \mathbf{Y} \mathbf{Q}_k \mathbf{v} = \mathbf{0}, \quad (34)$$

where $\mathbf{Q}_k = [\mathbf{e}, \theta_1, \theta_2, \dots, \theta_{k-1}]$. We consider the following two cases.

First, suppose that $\mathbf{Y}^T \mathbf{X} \beta \notin \text{range}(\mathbf{Y}^T \mathbf{Y} \mathbf{Q}_k)$. Rearranging (34) yields

$$\hat{\theta} = \frac{1}{1 + \psi} (\mathbf{Y}^T \mathbf{Y})^{-1} (\mathbf{Y}^T \mathbf{X} \beta - \mathbf{Y}^T \mathbf{Y} \mathbf{Q}_k \mathbf{v}). \quad (35)$$

We choose the dual variables ψ and \mathbf{v} so that $\hat{\boldsymbol{\theta}}$ is feasible for (32). It is easy to see that the conjugacy constraints are equivalent to $\mathbf{Q}_k^T \mathbf{Y}^T \mathbf{Y} \hat{\boldsymbol{\theta}} = \mathbf{0}$, which holds if and only if

$$\begin{aligned} \mathbf{0} &= \mathbf{Q}_k^T (\mathbf{Y}^T \mathbf{X} \boldsymbol{\beta} - \mathbf{Y}^T \mathbf{Y} \mathbf{Q}_k \mathbf{v}) \\ &= \mathbf{Q}_k^T \mathbf{Y}^T \mathbf{X} \boldsymbol{\beta} - \mathbf{Q}_k^T \mathbf{Y}^T \mathbf{Y} \mathbf{Q}_k \mathbf{v} \\ &= \mathbf{Q}_k^T \mathbf{Y}^T \boldsymbol{\beta} - n \mathbf{v}, \end{aligned}$$

where the last equality follows from the fact that $\mathbf{e}^T \mathbf{Y}^T \mathbf{Y} \mathbf{e} = \boldsymbol{\theta}_i^T \mathbf{Y}^T \mathbf{Y} \boldsymbol{\theta}_i = n$ for all $i = 1, 2, \dots, k-1$. It follows immediately that

$$\mathbf{v} = \frac{1}{n} \mathbf{Q}_k^T \mathbf{Y}^T \mathbf{X} \boldsymbol{\beta}. \quad (36)$$

Substituting (36) into (35) yields

$$\begin{aligned} \hat{\boldsymbol{\theta}} &= \frac{1}{1+\psi} \left((\mathbf{Y}^T \mathbf{Y})^{-1} \mathbf{Y}^T \mathbf{X} \boldsymbol{\beta} - \frac{1}{n} \mathbf{Q}_k \mathbf{Q}_k^T \mathbf{Y}^T \mathbf{X} \boldsymbol{\beta} \right) \\ &= \frac{1}{n(1+\psi)} \left(\mathbf{D}^{-1} \mathbf{Y}^T \mathbf{X} \boldsymbol{\beta} - \mathbf{Q}_k \mathbf{Q}_k^T \mathbf{Y}^T \mathbf{X} \boldsymbol{\beta} \right) \\ &= \frac{1}{n(1+\psi)} \left(\mathbf{I} - \mathbf{Q}_k \mathbf{Q}_k^T \mathbf{D} \right) \mathbf{D}^{-1} \mathbf{Y}^T \mathbf{X} \boldsymbol{\beta} \\ &= \frac{1}{n(1+\psi)} \mathbf{w}, \end{aligned} \quad (37)$$

where $\mathbf{D} = \frac{1}{n} \mathbf{Y}^T \mathbf{Y}$ and we choose $\psi \in \mathbf{R}$ so that $\hat{\boldsymbol{\theta}}^T \mathbf{D} \hat{\boldsymbol{\theta}} = 1$:

$$n(1+\psi) = \pm \sqrt{\mathbf{w}^T \mathbf{D} \mathbf{w}}. \quad (38)$$

To complete the argument, note that

$$\begin{aligned} \|\mathbf{Y} \hat{\boldsymbol{\theta}} - \mathbf{X} \boldsymbol{\beta}\|^2 &= n \mp \frac{2}{\sqrt{\mathbf{w}^T \mathbf{D} \mathbf{w}}} \boldsymbol{\beta}^T \mathbf{X}^T \mathbf{Y} (\mathbf{D}^{-1} - \mathbf{Q}_k \mathbf{Q}_k^T) \mathbf{Y}^T \mathbf{X} \boldsymbol{\beta} \\ &\quad + \boldsymbol{\beta}^T \mathbf{X}^T \mathbf{X} \boldsymbol{\beta}. \end{aligned}$$

Note further that the matrix $\mathbf{Y} \mathbf{Q}_k \mathbf{Q}_k^T \mathbf{Y}^T$ has decomposition

$$\begin{aligned} \mathbf{Y} \mathbf{Q}_k \mathbf{Q}_k^T \mathbf{Y}^T &= \mathbf{Y} \mathbf{e} \mathbf{e}^T \mathbf{Y}^T + \mathbf{Y} \boldsymbol{\theta}_1 \boldsymbol{\theta}_1^T \mathbf{Y}^T + \dots \\ &\quad + \mathbf{Y} \boldsymbol{\theta}_{k-1} \boldsymbol{\theta}_{k-1}^T \mathbf{Y}^T. \end{aligned}$$

The conjugacy of the columns of \mathbf{Q}_k implies that $\mathbf{Y} \mathbf{Q}_k \mathbf{Q}_k^T \mathbf{Y}^T$ has eigenvectors $\mathbf{Y} \boldsymbol{\theta}_1, \dots, \mathbf{Y} \boldsymbol{\theta}_{k-1}$, and $\mathbf{Y} \mathbf{e}$, each with eigenvalue n ; since $\text{rank}(\mathbf{Y} \mathbf{Q}_k \mathbf{Q}_k^T \mathbf{Y}^T) = k$, all remaining eigenvalues of $\mathbf{Y} \mathbf{Q}_k \mathbf{Q}_k^T \mathbf{Y}^T$ must be equal to 0. Moreover, for any $\mathbf{z} = \mathbf{Y} \boldsymbol{\theta}_i$, $i = 1, 2, \dots, k-1$, or $\mathbf{z} = \mathbf{Y} \mathbf{e}$, we have

$$\mathbf{Y} (\mathbf{D}^{-1} - \mathbf{Q}_k \mathbf{Q}_k^T) \mathbf{Y}^T \mathbf{z} = (n - n) \mathbf{z} = \mathbf{0}.$$

The matrix \mathbf{D}^{-1} is a positive definite diagonal matrix, with (i, i) -th entry equal to $|C_i|/n$ where $|C_i|$ denotes the number of observations belonging to class i ; this implies that $\mathbf{Y} \mathbf{D}^{-1} \mathbf{Y}^T$ is positive semidefinite. This establishes that the matrix $\mathbf{Y} (\mathbf{D}^{-1} - \mathbf{Q}_k \mathbf{Q}_k^T) \mathbf{Y}^T$ is positive semidefinite and thus $\|\mathbf{Y} \boldsymbol{\theta} - \mathbf{X} \boldsymbol{\beta}\|^2$ is minimized by $\hat{\boldsymbol{\theta}}$ with $\psi = +\sqrt{\mathbf{w}^T \mathbf{D} \mathbf{w}}/n - 1$.

Second, suppose that $\mathbf{Y}^T \mathbf{X} \boldsymbol{\beta} \in \text{range}(\mathbf{Y}^T \mathbf{Y} \mathbf{Q}_k)$. This implies that there exists some $\mathbf{v} \in \mathbf{R}^k$ such that

$$\mathbf{Y}^T \mathbf{X} \boldsymbol{\beta} = \mathbf{Y}^T \mathbf{Y} \mathbf{Q}_k \mathbf{v}.$$

Substituting into the objective of (32), we see that

$$\begin{aligned} \|\mathbf{Y} \boldsymbol{\theta} - \mathbf{X} \boldsymbol{\beta}\|^2 &= \boldsymbol{\theta}^T \mathbf{Y}^T \mathbf{Y} \boldsymbol{\theta} - 2 \boldsymbol{\theta}^T \mathbf{Y}^T \mathbf{X} \boldsymbol{\beta} + \boldsymbol{\beta}^T \mathbf{X}^T \mathbf{X} \boldsymbol{\beta} \\ &= n - 2 \boldsymbol{\theta}^T \mathbf{Y}^T \mathbf{Y} \mathbf{Q}_k \mathbf{v} + \boldsymbol{\beta}^T \mathbf{X}^T \mathbf{X} \boldsymbol{\beta} \\ &= n + \boldsymbol{\beta}^T \mathbf{X}^T \mathbf{X} \boldsymbol{\beta} \end{aligned}$$

for every feasible solution $\boldsymbol{\theta}$ of (32). This implies that every feasible solution of (32) is also optimal in this case. In particular, $\hat{\boldsymbol{\theta}}$ given by (37) is feasible for (32) and, therefore, optimal.

References

- Z. Allen-Zhu and L. Orecchia. Linear coupling: An ultimate unification of gradient and mirror descent. *arXiv preprint arXiv:1407.1537*, 2014.
- B. Ames and M. Hong. Alternating direction method of multipliers for penalized zero-variance discriminant analysis. *Computational Optimization and Applications*, 64(3):725–754, 2016.
- A. Beck and M. Teboulle. A fast iterative shrinkage-thresholding algorithm for linear inverse problems. *SIAM journal on imaging sciences*, 2(1):183–202, 2009.
- S. Boyd, N. Parikh, E. Chu, B. Peleato, and J. Eckstein. Distributed optimization and statistical learning via the alternating direction method of multipliers. *Foundations and Trends® in Machine Learning*, 3(1):1–122, 2011.
- S. Bubeck, Y. T. Lee, and M. Singh. A geometric alternative to Nesterov’s accelerated gradient descent. *arXiv preprint arXiv:1506.08187*, 2015.
- T. Cai and W. Liu. A direct estimation approach to sparse linear discriminant analysis. *Journal of the American Statistical Association*, 106(496), 2011.
- L. Clemmensen, M. Hansen, J. Frisvad, and B. Ersbøll. A method for comparison of growth media in objective identification of penicillium based

- on multi-spectral imaging. *Journal of Microbiological Methods*, 69(2):249–255, 2007.
- L. Clemmensen, T. Hastie, D. Witten, and B. Ersbøll. Sparse discriminant analysis. *Technometrics*, 53(4), 2011.
- W. Deng and W. Yin. On the global and linear convergence of the generalized alternating direction method of multipliers. *Journal of Scientific Computing*, pages 1–28, 2012.
- G. Einarsson, J. N. Jensen, R. R. Paulsen, H. Einarsson, B. K. Ersbøll, A. B. Dahl, and L. B. Christensen. Foreign object detection in multispectral x-ray images of food items using sparse discriminant analysis. In *Scandinavian Conference on Image Analysis*, pages 350–361. Springer, 2017.
- J. Fan and Y. Fan. High dimensional classification using features annealed independence rules. *Annals of Statistics*, 36(6):2605–2637, 2008.
- N. Flammarion and F. Bach. From averaging to acceleration, there is only a step-size. *arXiv preprint arXiv:1504.01577*, 2015.
- G. H. Golub and C. F. Van Loan. *Matrix Computations*, volume 3. JHU Press, 2013.
- T. Hastie, R. Tibshirani, and A. Buja. Flexible discriminant analysis by optimal scoring. *Journal of the American Statistical Association*, 89(428):1255–1270, 1994.
- T. Hastie, R. Tibshirani, and J. J. H. Friedman. *The Elements of Statistical Learning*. Springer New York, 2013.
- T. Hastie, R. Tibshirani, and M. Wainwright. *Statistical Learning with Sparsity: the Lasso and Generalizations*. CRC Press, 2015.
- E. Keogh, X. Xi, L. Wei, and C. A. Ratanamahatana. The UCR time series classification/clustering homepage, 2006.
- L. Lessard, B. Recht, and A. Packard. Analysis and design of optimization algorithms via integral quadratic constraints. *SIAM Journal on Optimization*, 26(1):57–95, 2016.
- Q. Mai and H. Zou. A note on the connection and equivalence of three sparse linear discriminant analysis methods. *Technometrics*, 55(2):243–246, 2013.
- Q. Mai and H. Zou. Multiclass sparse discriminant analysis. *arXiv preprint arXiv:1504.05845v1*, 2015.
- Q. Mai, M. Yuan, and H. Zou. A direct approach to sparse discriminant analysis in ultra-high dimensions. *Biometrika*, 99:29–42, 2012.
- B. Matérn. *Spatial variation*, volume 36. Springer Science & Business Media, 2013.
- Y. Nesterov. A method of solving a convex programming problem with convergence rate $o(1/k^2)$. In *Soviet Mathematics Doklady*, volume 27, pages 372–376, 1983.
- Y. Nesterov. Smooth minimization of non-smooth functions. *Mathematical programming*, 103(1):127–152, 2005.
- Y. Nesterov. Gradient methods for minimizing composite functions. *Mathematical Programming*, 140(1):125–161, 2013.
- J. Nocedal and S. Wright. *Numerical optimization*. Springer Science & Business Media, 2006.
- B. O’Donoghue and E. Candes. Adaptive restart for accelerated gradient schemes. *Foundations of Computational Mathematics*, 15(3):715–732, 2015.
- N. Parikh and S. P. Boyd. Proximal algorithms. *Foundations and Trends in optimization*, 1(3):127–239, 2014.
- J. Shao, Y. Wang, X. Deng, and S. Wang. Sparse linear discriminant analysis by thresholding for high dimensional data. *The Annals of Statistics*, 39(2):1241–1265, 2011.
- W. Su, S. Boyd, and E. Candes. A differential equation for modeling nesterov’s accelerated gradient method: Theory and insights. In *Advances in Neural Information Processing Systems*, pages 2510–2518, 2014.
- R. Tibshirani, T. Hastie, B. Narasimhan, and G. Chu. Class prediction by nearest shrunken centroids, with applications to dna microarrays. *Statistical Science*, pages 104–117, 2003.
- P. Tseng. On accelerated proximal gradient methods for convex-concave optimization. submitted to *SIAM Journal on Optimization*, 2008.
- D. M. Witten and R. Tibshirani. Penalized classification using Fisher’s linear discriminant. *Journal of the Royal Statistical Society: Series B (Statistical Methodology)*, 73(5):753–772, 2011.
- M. Wu, L. Zhang, Z. Wang, D. Christiani, and X. Lin. Sparse linear discriminant analysis for simultaneous testing for the significance of a gene

set/pathway and gene selection. *Bioinformatics*, 25:1145–1151, 2008.

H. Zou and T. Hastie. Regularization and variable selection via the elastic net. *Journal of the Royal Statistical Society: Series B (Statistical Methodology)*, 67(2):301–320, 2005.

Dataset	Measures	SDAP	SDAAP	SDAD	SZVD	SDA
$p = 500$	numErr	9.50 (11.52)	9.00 (11.63)	6.75 (5.95)	1.55 (2.14)	113.75 (13.04)
$r = 0$	fracErr	0.02 (0.02)	0.02 (0.02)	0.01 (0.01)	0.00 (0.00)	0.23 (0.03)
$K = 2$	feats	81.90 (36.86)	88.55 (36.04)	91.45 (30.93)	135.15 (25.09)	8.00 (0.00)
	fracFeats	0.16 (0.07)	0.18 (0.07)	0.18 (0.06)	0.27 (0.05)	0.02 (0.00)
	time	31.57 (2.46)	24.87 (1.43)	131.32 (2.18)	59.62 (12.12)	22.76 (1.28)
$p = 500$	numErr	6.85 (7.68)	7.35 (9.83)	7.95 (5.69)	0.75 (0.85)	117.50 (16.38)
$r = 0.1$	fracErr	0.01 (0.02)	0.01 (0.02)	0.02 (0.01)	0.00 (0.00)	0.24 (0.03)
$K = 2$	feats	83.60 (33.42)	89.85 (36.61)	77.25 (27.37)	139.85 (16.73)	8.00 (0.00)
	fracFeats	0.17 (0.07)	0.18 (0.07)	0.15 (0.05)	0.28 (0.03)	0.02 (0.00)
	time	49.73 (7.95)	27.46 (2.10)	132.95 (0.95)	60.76 (13.60)	23.18 (1.09)
$p = 500$	numErr	1.90 (2.90)	1.90 (3.21)	0.45 (0.83)	0.00 (0.00)	94.10 (25.14)
$r = 0.5$	fracErr	0.00 (0.01)	0.00 (0.01)	0.00 (0.00)	0.00 (0.00)	0.19 (0.05)
$K = 2$	feats	75.25 (29.70)	85.95 (36.60)	71.65 (15.16)	143.40 (14.25)	8.00 (0.00)
	fracFeats	0.15 (0.06)	0.17 (0.07)	0.14 (0.03)	0.29 (0.03)	0.02 (0.00)
	time	214.63 (27.34)	37.01 (3.90)	130.33 (1.80)	56.28 (8.51)	22.86 (1.43)
$p = 500$	numErr	4.80 (20.30)	4.80 (21.00)	0.00 (0.00)	0.00 (0.00)	19.65 (20.88)
$r = 0.9$	fracErr	0.01 (0.04)	0.01 (0.04)	0.00 (0.00)	0.00 (0.00)	0.04 (0.04)
$K = 2$	feats	51.70 (25.75)	75.65 (35.88)	94.00 (9.28)	164.65 (12.91)	8.00 (0.00)
	fracFeats	0.10 (0.05)	0.15 (0.07)	0.19 (0.02)	0.33 (0.03)	0.02 (0.00)
	time	194.13 (25.24)	28.80 (3.11)	135.31 (1.58)	60.82 (17.93)	23.96 (2.30)
$p = 500$	numErr	32.60 (14.55)	25.70 (16.15)	9.15 (6.11)	11.95 (7.06)	191.45 (24.85)
$r = 0$	fracErr	0.03 (0.01)	0.03 (0.02)	0.01 (0.01)	0.01 (0.01)	0.19 (0.02)
$K = 4$	feats	252.80 (68.10)	279.05 (66.02)	522.95 (14.24)	426.50 (42.82)	69.05 (0.22)
	fracFeats	0.17 (0.05)	0.19 (0.04)	0.35 (0.01)	0.28 (0.03)	0.05 (0.00)
	time	33.29 (2.46)	65.23 (3.02)	424.30 (4.71)	476.76 (90.16)	805.62 (37.15)
$p = 500$	numErr	44.35 (17.85)	33.80 (11.99)	5.30 (2.94)	28.55 (29.26)	245.05 (23.44)
$r = 0.1$	fracErr	0.04 (0.02)	0.03 (0.01)	0.01 (0.00)	0.03 (0.03)	0.25 (0.02)
$K = 4$	feats	262.80 (60.28)	296.20 (54.55)	540.55 (18.04)	381.80 (85.53)	69.00 (0.00)
	fracFeats	0.18 (0.04)	0.20 (0.04)	0.36 (0.01)	0.25 (0.06)	0.05 (0.00)
	time	87.99 (13.43)	71.69 (4.08)	430.38 (7.55)	467.19 (86.11)	787.50 (58.68)
$p = 500$	numErr	7.25 (5.95)	3.85 (3.07)	0.00 (0.00)	3.75 (7.30)	153.50 (28.41)
$r = 0.5$	fracErr	0.01 (0.01)	0.00 (0.00)	0.00 (0.00)	0.00 (0.01)	0.15 (0.03)
$K = 4$	feats	263.65 (21.94)	309.00 (21.22)	597.80 (23.67)	361.85 (68.06)	69.00 (0.00)
	fracFeats	0.18 (0.01)	0.21 (0.01)	0.4 (0.02)	0.24 (0.05)	0.05 (0.00)
	time	352.05 (29.60)	90.43 (8.89)	444.74 (10.22)	541.43 (144.59)	804.96 (52.84)
$p = 500$	numErr	3.40 (6.06)	3.40 (7.38)	0.00 (0.00)	25.00 (77.45)	4.70 (5.39)
$r = 0.9$	fracErr	0.00 (0.01)	0.00 (0.01)	0.00 (0.00)	0.02 (0.08)	0.00 (0.01)
$K = 4$	feats	223.70 (127.38)	193.40 (33.13)	796.20 (52.95)	355.25 (135.89)	69.00 (0.00)
	fracFeats	0.15(0.08)	0.13 (0.02)	0.53(0.04)	0.24 (0.09)	0.05 (0.00)
	time	343.42 (21.42)	72.44 (6.31)	510.91 (11.66)	446.70 (158.79)	785.33 (32.50)

Table 3: Results for Type 1 synthetic data. All results are listed in the format “mean (standard deviation)”. In all experiments, $n_{train} = 25K$ and $n_{test} = 250K$.

Dataset	Measures	SDAP	SDAAP	SDAD	SZVD	SDA
$p = 500$	numErr	9.50 (11.52)	9.00 (11.63)	6.75 (5.95)	1.55 (2.14)	113.75 (13.04)
$r = 0$	fracErr	0.02 (0.02)	0.02 (0.02)	0.01 (0.01)	0.00 (0.00)	0.23 (0.03)
$K = 2$	feats	81.90 (36.86)	88.55 (36.04)	91.45 (30.93)	135.15 (25.09)	8.00 (0.00)
	fracFeats	0.16 (0.07)	0.18 (0.07)	0.18 (0.06)	0.27 (0.05)	0.02 (0.00)
	time	28.84 (2.26)	25.38 (1.41)	132.87 (1.27)	62.44 (12.85)	23.16 (1.12)
$p = 500$	numErr	8.95 (10.77)	7.40 (8.64)	8.20 (5.86)	3.15 (5.56)	111.05 (15.26)
$r = 0.1$	fracErr	0.02 (0.02)	0.01 (0.02)	0.02 (0.01)	0.01 (0.01)	0.22 (0.03)
$K = 2$	feats	93.95 (48.19)	94.75 (34.30)	86.45 (23.69)	132.80 (28.13)	8.00 (0.00)
	fracFeats	0.19 (0.10)	0.19 (0.07)	0.17 (0.05)	0.27 (0.06)	0.02 (0.00)
	time	28.36 (2.37)	24.67 (1.42)	133.24 (1.13)	60.39 (10.04)	23.02 (0.99)
$p = 500$	numErr	25.50 (13.74)	19.95 (9.98)	22.55 (8.11)	12.80 (7.88)	116.55 (18.14)
$r = 0.5$	fracErr	0.05 (0.03)	0.04 (0.02)	0.05 (0.02)	0.03 (0.02)	0.23 (0.04)
$K = 2$	feats	72.25 (36.20)	81.85 (27.66)	75.25 (18.45)	136.45 (35.10)	8.00 (0.00)
	fracFeats	0.14 (0.07)	0.16 (0.06)	0.15 (0.04)	0.27 (0.07)	0.02 (0.00)
	time	31.44 (2.76)	26.17 (1.70)	128.89 (1.97)	72.51 (17.74)	24.74 (1.15)
$p = 500$	numErr	99.50 (12.53)	99.15 (11.48)	110.25 (11.64)	116.15 (16.75)	133.75 (16.25)
$r = 0.9$	fracErr	0.20 (0.03)	0.20 (0.02)	0.22 (0.02)	0.23 (0.03)	0.27 (0.03)
$K = 2$	feats	59.65 (34.47)	66.85 (31.87)	92.10 (22.81)	132.90 (22.27)	8.00 (0.00)
	fracFeats	0.12 (0.07)	0.13 (0.06)	0.18 (0.05)	0.27 (0.04)	0.02 (0.00)
	time	51.49 (7.20)	66.02 (2.43)	116.43 (4.31)	120.82 (20.72)	30.57 (2.10)
$p = 500$	numErr	32.60 (14.55)	25.70 (16.15)	9.15 (6.11)	11.95 (7.06)	191.45 (24.85)
$r = 0$	fracErr	0.03 (0.01)	0.03 (0.02)	0.01 (0.01)	0.01 (0.01)	0.19 (0.02)
$K = 4$	feats	252.80 (68.10)	279.05 (66.02)	522.95 (14.24)	426.50 (42.82)	69.05 (0.22)
	fracFeats	0.17 (0.05)	0.19 (0.05)	0.35 (0.01)	0.28 (0.03)	0.05 (0.00)
	time	36.22 (3.18)	65.45 (3.14)	427.83 (7.06)	443.24 (77.38)	705.49 (67.77)
$p = 500$	numErr	43.00 (19.26)	28.45 (15.98)	10.75 (4.72)	18.58 (9.36)	196.65 (25.32)
$r = 0.1$	fracErr	0.04 (0.02)	0.03 (0.02)	0.01 (0.00)	0.02 (0.01)	0.20 (0.03)
$K = 4$	feats	253.35 (74.60)	299.60 (83.63)	537.20 (24.01)	419.53 (45.13)	69.00 (0.00)
	fracFeats	0.17(0.05)	0.20 (0.06)	0.36 (0.02)	0.28 (0.03)	0.05 (0.00)
	time	36.90 (2.38)	67.01 (2.33)	430.11 (7.51)	475.23 (83.24)	742.81 (46.20)
$p = 500$	numErr	89.80 (20.86)	84.70 (22.96)	62.55 (10.24)	125.90 (93.66)	230.80 (25.47)
$r = 0.5$	fracErr	0.09 (0.02)	0.08 (0.02)	0.06 (0.01)	0.13 (0.09)	0.23 (0.03)
$K = 4$	feats	259.95 (52.78)	281.00 (47.87)	560.85 (20.69)	383.35 (68.22)	69.05 (0.22)
	fracFeats	0.17 (0.04)	0.19 (0.03)	0.37 (0.01)	0.26 (0.05)	0.05 (0.00)
	time	41.62 (4.27)	72.10 (2.82)	415.59 (5.75)	483.74 (121.77)	854.26 (51.16)
$p = 500$	numErr	368.10 (37.14)	366.20 (29.92)	453.15 (32.76)	502.65 (29.87)	391.85 (18.91)
$r = 0.9$	fracErr	0.37 (0.04)	0.37 (0.03)	0.45 (0.03)	0.50 (0.03)	0.39 (0.02)
$K = 4$	feats	189.25 (82.78)	269.55 (96.00)	867.25 (46.11)	416.20 (55.93)	69.25 (0.44)
	fracFeats	0.13 (0.06)	0.18 (0.06)	0.58 (0.03)	0.28 (0.04)	0.05 (0.00)
	time	103.07 (6.48)	100.21 (7.28)	400.24 (11.51)	1034.96 (148.44)	1096.82 (118.89)

Table 4: Results for Type 2 synthetic data. All results are listed in the format “mean (standard deviation)”. In all experiments, $n_{train} = 25K$ and $n_{test} = 250K$.

Dataset	Measures	SDAP	SDAPbt	SDAAP	SDAAPbt	SDAD
$p = 500$	numErr	10.85 (10.94)	9.70 (10.09)	12.60 (11.18)	5.60 (10.29)	12.25 (4.40)
$r = 0$	fracErr	0.02 (0.02)	0.02 (0.02)	0.03 (0.02)	0.01 (0.02)	0.02 (0.01)
$K = 2$	feats	76.65 (35.14)	75.85 (27.13)	68.95 (26.70)	116.10 (41.37)	63.20 (4.35)
	fracFeats	0.15 (0.07)	0.15 (0.05)	0.14 (0.05)	0.23 (0.08)	0.13 (0.01)
	time	67.88 (3.22)	833.49 (14.24)	50.10 (0.66)	341.87 (5.57)	112.16 (0.72)
$p = 500$	numErr	6.90 (8.38)	5.45 (7.57)	10.45 (10.78)	3.70 (5.89)	10.40 (3.59)
$r = 0.1$	fracErr	0.01 (0.02)	0.01 (0.02)	0.02 (0.02)	0.01 (0.01)	0.02 (0.01)
$K = 2$	feats	78.95 (28.13)	90.45 (37.62)	70.65 (25.99)	106.50 (32.13)	63.40 (5.47)
	fracFeats	0.16 (0.06)	0.18 (0.08)	0.14 (0.05)	0.21 (0.06)	0.13 (0.01)
	time	107.35 (16.69)	712.61 (12.68)	54.99 (3.22)	380.27 (10.02)	124.90 (2.82)
$p = 500$	numErr	1.45 (2.16)	1.40 (2.19)	2.35 (2.78)	0.70 (1.63)	0.50 (0.83)
$r = 0.5$	fracErr	0.00 (0.00)	0.00 (0.00)	0.00 (0.01)	0.00 (0.00)	0.00 (0.00)
$K = 2$	feats	73.95 (27.71)	77.05 (30.09)	67.15 (26.89)	107.10 (40.63)	68.30 (6.14)
	fracFeats	0.15 (0.06)	0.15 (0.06)	0.13 (0.05)	0.21 (0.08)	0.14 (0.01)
	time	608.50 (57.66)	777.07 (40.32)	83.02 (8.91)	382.49 (8.39)	108.38 (0.91)
$p = 500$	numErr	0.00 (0.00)	0.00 (0.00)	0.00 (0.00)	0.05 (0.22)	0.00 (0.00)
$r = 0.9$	fracErr	0.00 (0.00)	0.00 (0.00)	0.00 (0.00)	0.00 (0.00)	0.00 (0.00)
$K = 2$	feats	83.95 (25.46)	83.95 (25.46)	127.45 (55.30)	126.95 (61.77)	94.00 (9.28)
	fracFeats	0.17 (0.05)	0.17 (0.05)	0.25 (0.11)	0.25 (0.12)	0.19 (0.02)
	time	373.35 (29.85)	429.37 (24.18)	86.49 (6.60)	387.19 (24.06)	127.02 (3.90)
$p = 500$	numErr	15.30 (9.82)	15.30 (9.82)	23.10 (12.17)	15.60 (11.21)	9.15 (6.11)
$r = 0$	fracErr	0.02 (0.01)	0.02 (0.01)	0.02 (0.01)	0.02 (0.01)	0.01 (0.01)
$K = 4$	feats	326.20 (101.56)	326.20 (101.56)	276.65 (91.62)	329.70 (86.63)	522.95 (14.24)
	fracFeats	0.22 (0.07)	0.22(0.07)	0.18 (0.06)	0.22 (0.06)	0.35 (0.01)
	time	62.48 (2.42)	1276.92 (46.92)	106.86 (2.99)	1151.02 (37.41)	613.81 (19.02)
$p = 500$	numErr	33.95 (15.17)	33.95 (15.17)	29.55 (17.29)	23.75 (32.70)	5.30 (2.94)
$r = 0.1$	fracErr	0.03 (0.02)	0.03 (0.02)	0.03 (0.02)	0.02 (0.03)	0.01 (0.00)
$K = 4$	feats	287.70 (65.17)	287.70 (65.17)	303.70 (76.70)	384.20 (108.67)	540.55 (18.04)
	fracFeats	0.19 (0.04)	0.19 (0.04)	0.20 (0.05)	0.26 (0.07)	0.36(0.01)
	time	209.76 (24.47)	1509.73 (55.24)	133.22 (6.37)	1124.25 (39.43)	453.65 (6.82)
$p = 500$	numErr	3.55 (3.62)	3.55 (3.62)	3.85 (3.07)	3.15 (3.62)	0.00 (0.00)
$r = 0.5$	fracErr	0.00 (0.00)	0.00 (0.00)	0.00 (0.00)	0.00 (0.00)	0.00 (0.00)
$K = 4$	feats	302.50 (30.84)	302.50 (30.84)	309.00 (21.22)	341.80 (69.80)	597.80 (23.67)
	fracFeats	0.20 (0.02)	0.20 (0.02)	0.21 (0.01)	0.23(0.05)	0.40 (0.02)
	time	702.73 (29.81)	1108.16 (33.74)	160.39 (14.50)	1092.52 (39.17)	508.87 (15.70)
$p = 500$	numErr	7.50 (14.76)	3.60 (6.59)	3.40 (7.38)	2.45 (3.41)	0.00 (0.00)
$r = 0.9$	fracErr	0.01 (0.01)	0.00 (0.01)	0.00 (0.01)	0.00 (0.00)	0.00 (0.00)
$K = 4$	feats	202.35 (112.25)	191.80 (86.54)	193.40 (33.13)	198.50 (62.15)	796.20 (52.95)
	fracFeats	0.13 (0.07)	0.13 (0.06)	0.13 (0.02)	0.13 (0.04)	0.53 (0.04)
	time	519.18 (36.52)	564.09 (44.68)	91.06 (8.90)	633.67 (17.40)	593.18 (9.42)

Table 5: Results for Type 1 synthetic data. All results are listed in the format “mean (standard deviation)”. In all experiments, $n_{train} = 25K$ and $n_{test} = 250K$. We used fixed score vectors given by the projection of $\theta = (1, 2, \dots, K)$ on to the feasible region of (2), as opposed to the randomly sampled initial scoring vectors used in the simulations summarized in Tables 3 and 4.

Dataset	Measures	SDAP	SDAPbt	SDAAP	SDAAPbt	SDAD
$p = 500$	numErr	10.85 (10.94)	9.70 (10.09)	12.60 (11.18)	5.60 (10.29)	12.25 (4.40)
$r = 0$	fracErr	0.02 (0.02)	0.02 (0.02)	0.03 (0.02)	0.01 (0.02)	0.02 (0.01)
$k = 2$	feats	76.65 (35.14)	75.85 (27.13)	68.95 (26.70)	116.10 (41.37)	63.20 (4.35)
	fracFeats	0.15 (0.07)	0.15 (0.05)	0.14 (0.05)	0.23 (0.08)	0.13 (0.01)
	time	65.89 (3.03)	732.29 (59.02)	52.96 (2.33)	330.48 (9.44)	111.11 (1.58)
$p = 500$	numErr	13.00 (11.02)	8.50 (9.90)	14.30 (12.07)	7.45 (12.43)	13.20 (5.19)
$r = 0.1$	fracErr	0.03 (0.02)	0.02 (0.02)	0.03 (0.02)	0.01 (0.02)	0.03 (0.01)
$k = 2$	feats	69.70 (25.69)	87.00 (35.76)	66.95 (26.05)	117.55 (40.23)	64.15 (4.90)
	fracFeats	0.14 (0.05)	0.17 (0.07)	0.13 (0.05)	0.24 (0.08)	0.13 (0.01)
	time	63.54 (3.94)	713.47 (32.68)	50.43 (0.96)	329.37 (12.36)	111.79 (1.97)
$p = 500$	numErr	24.80 (12.76)	24.25 (12.49)	23.50 (10.19)	19.70 (10.05)	24.95 (7.02)
$r = 0.5$	fracErr	0.05 (0.03)	0.05 (0.02)	0.05 (0.02)	0.04 (0.02)	0.05 (0.01)
$k = 2$	feats	71.75 (25.73)	73.60 (25.64)	68.90 (21.12)	97.10 (39.14)	64.60 (6.32)
	fracFeats	0.14 (0.05)	0.15 (0.05)	0.14 (0.04)	0.19 (0.08)	0.13 (0.01)
	time	70.54 (4.17)	724.34 (34.87)	53.17 (1.36)	339.85 (13.03)	110.70 (2.14)
$p = 500$	numErr	95.00 (10.72)	94.35 (10.65)	96.25 (10.85)	97.80 (10.34)	110.05 (11.38)
$r = 0.9$	fracErr	0.19 (0.02)	0.19 (0.02)	0.19 (0.02)	0.20 (0.02)	0.22 (0.02)
$k = 2$	feats	67.55 (34.45)	71.80 (29.58)	67.15 (26.39)	79.25 (32.91)	82.90 (9.97)
	fracFeats	0.14 (0.07)	0.14 (0.06)	0.13 (0.05)	0.16 (0.07)	0.17 (0.02)
	time	129.85 (13.63)	818.49 (36.75)	68.90 (2.30)	394.60 (13.24)	100.49 (2.36)
$p = 500$	numErr	15.30 (9.82)	15.30 (9.82)	23.10 (12.17)	15.60 (11.21)	9.15 (6.11)
$r = 0$	fracErr	0.02 (0.01)	0.02 (0.01)	0.02 (0.01)	0.02 (0.01)	0.01 (0.01)
$k = 4$	feats	326.20 (101.56)	326.20 (101.56)	276.65 (91.62)	329.70 (86.63)	522.95 (14.24)
	fracFeats	0.22 (0.07)	0.22 (0.07)	0.18 (0.06)	0.22 (0.06)	0.35 (0.01)
	time	59.29 (3.11)	1286.99 (65.08)	103.05 (2.83)	1109.64 (34.96)	439.55 (6.42)
$p = 500$	numErr	24.45 (19.18)	22.21 (16.80)	25.25 (12.09)	28.85 (19.55)	10.75 (4.72)
$r = 0.1$	fracErr	0.02 (0.02)	0.02 (0.02)	0.03 (0.01)	0.03 (0.02)	0.01 (0.00)
$k = 4$	feats	336.20 (123.02)	341.05 (124.41)	310.10 (110.61)	357.25 (106.35)	537.20 (24.01)
	fracFeats	0.22 (0.08)	0.23 (0.08)	0.21 (0.07)	0.24 (0.07)	0.36 (0.02)
	time	65.46 (2.40)	1288.82 (69.13)	109.13 (2.55)	1065.56 (40.87)	438.60 (5.75)
$p = 500$	numErr	81.00 (15.61)	81.00 (15.61)	88.25 (22.15)	88.05 (30.30)	62.55 (10.24)
$r = 0.5$	fracErr	0.08 (0.02)	0.08 (0.02)	0.09 (0.02)	0.09 (0.03)	0.06 (0.01)
$k = 4$	feats	281.05 (25.36)	281.05 (25.36)	289.75 (61.76)	334.65 (95.71)	560.85 (20.69)
	fracFeats	0.19 (0.02)	0.19 (0.02)	0.19 (0.04)	0.22 (0.06)	0.37 (0.01)
	time	71.26 (5.40)	1158.02 (60.57)	113.39 (4.88)	1098.42 (38.58)	413.33 (6.68)
$p = 500$	numErr	359.60 (20.36)	366.55 (18.10)	357.30 (17.17)	371.90 (24.76)	453.15 (32.76)
$r = 0.9$	fracErr	0.36 (0.02)	0.37 (0.02)	0.36 (0.02)	0.37 (0.02)	0.45 (0.03)
$k = 4$	feats	297.95 (95.81)	269.95 (118.74)	243.00 (50.40)	242.15 (81.42)	867.25 (46.11)
	fracFeats	0.20 (0.06)	0.18 (0.08)	0.16 (0.03)	0.16 (0.05)	0.58 (0.03)
	time	136.56 (8.61)	1365.36 (90.77)	132.12 (7.84)	1197.91 (112.01)	445.67 (10.00)

Table 6: Results for Type 2 synthetic data. All results are listed in the format “mean (standard deviation)”. In all experiments, $n_{train} = 25K$ and $n_{test} = 250K$. We used fixed score vectors given by the projection of $\theta = (1, 2, \dots, K)$ on to the feasible region of (2), as opposed to the randomly sampled initial scoring vectors used in the simulations summarized in Tables 3 and 4.